

Central European Journal of Chemistry

Pressure induced structural phase transitions—A review

Review Article

Purvee Bhardwaj*, Sadhna Singh

High pressure Research Laboratory, Department of Physics, Barkatullah University, Bhopal 462026, India

Received 11 January 2012; Accepted 18 May 2012

Abstract: The contemporary status of experimental as well as theoretical advances within the special view of structural phase transitions is reviewed. A brief outline of phase transitions and its classification is presented first. High-pressure experimental techniques developed for studying the structural phase transitions and elastic properties are reviewed. The complete set of theoretical and experimental data obtained is for the group II-IV alkaline earth chalcogenides. Here the authors review the currently used calculations and high-pressure behavior of these materials and the theoretical work that has been done on them.

Keywords: Structural Phase transition • High pressure • Elastic properties • Alkaline earth © Versita Sp. z o.o.

1. Introduction

The solid-state materials are found to exhibit many important properties out of which their phase transition and anharmonic properties occur due to the change of either pressure or temperatures or both. The studies of high-pressure techniques are important in understanding the physics of solids, and they are used in all branches of science. We can say that the high pressure creates the same phenomenon that takes place during the cohesion of solids. The compression is the main result of the pressure-induced changes in the properties of matter, which are the result of compression as the constituent particles (molecules, ions or atoms) are brought closure under pressure. The increased overlap of the electron cloud leads to a rearrangement of the band structure, which is reflected in the changes in the optical, electrical and many other physical properties. The Gibb's free energy or more generally free energy of the system varies with pressure, and at high pressure often assumes minimum for a spiral arrangement of particles different from the initial, resulting in a phase transition. The application of pressure stabilizes the unusual valency states, hinders diffusion and dissociation. It affects the kinetics of chemical reactions and phase transitions, provides new reaction paths, and modifies mechanical properties of engineering materials. The pressure induced

phase transition results in a new atomic arrangement. The pressure as a thermodynamic variable has offered many opportunities for basic research in the various disciplines of science, and also found numerous practical applications. High pressures are encountered from deep down in the earth to astro-physical objects. In materials science, the effect of pressure on materials helps to unravel the mysteries of the constituents of planetary bodies to deep down in the earth. In applied field like simulation of the reactor accidents, designing of inertial confinement fusion schemes and for understanding rock mechanical effects of shock propagation in earth due to nuclear explosion, the pressure versus volume relation of condensed matter are a vital input [1-3].

Materials come under high pressures in both natural and manmade explosions. High pressures may also be applied to small laboratory samples in a controlled manner using devices such as the diamond anvil cell (DAC). The static pressure applied in a DAC is a continuously variable parameter, which can be used for systematic studies of the properties of solids as a function of the interatomic distances. The continuous advancement and development of the diamond anvil cell (DAC) technology over the last few decades has opened a wide field of high-pressure science. This continuous advancement in pressure generating devices upper limit of pressure

^{*} E-mail: purveebhardwaj@gmail.com

in laboratories is increasing. Higher pressures are produced in laboratories using small commercial devices and further advancements are continuing for rising its limits. The investigation of different phenomena such as phase transition, structural changes due to strong compression and other changes in crystal structure are becoming important when the experimental techniques are providing better access and theoretical considerations are getting highly developed [4]. Most of the researchers in the late 80s came to conclusion that under pressure the materials take up high symmetry structure of increasing coordination number. But, the previously unexpected lower symmetry phases have been shown at intermediate pressure by experimentalists. The increasing sophistication and advancement in both experimental level with XRD studies and theoretical level with data analysis could provide better understanding of the structural unstabilities under pressure [5,6]. Now the contemporary high resolution data are subjected to more rigorous analysis techniques, allowing the discovery of earlier undetected symmetry break down distortions [2].

Besides these studies there are several theoretical studies based on *ab-initio* calculations which are available on number of compounds revealing electronic structures of these compounds. With the availability of modern computational facilities and advanced methodology it is now possible to calculate accurate energies of compounds. Minimum input data is required for calculation of total energies of solids in first principle calculations. With the knowledge of atomic number of the atoms, accurate energies can be calculated and the small energies difference of a few meV can also be calculated.

Now a number of ab-initio calculations are available on theoretical front. The ab-initio calculation has been performed for II-IV and III-V compounds to study the structural mechanical and thermal properties under pressure [7]. In most of the cases in the local density approximation the accuracy of total energies is sufficient to predict the structure at a given pressure with the lowest free energy. Most of the calculations are being performed at zero temperature. New ab-initio molecular dynamic methods give a better resolution for the structures and transformation mechanisms during the structural transition. Comparison of free energies of various possible phases provides us information about relative stability of structures and phase transition mechanism. Phenomenological lattice dynamical models, which are based on interatomic forces, are suitable for computating interaction energies to determine the actual stable structure and relative stability of structures.

The present review work is related with the highpressure phases of II-IV group. The present group of materials have two valence per atom. These materials have many resemblances at the normal conditions and under applied pressure. Consequently they may be considered as a group of compounds. The occurrence of first order phase transition in these materials involves a sudden change in volume and elastic constants.

The alkaline earth chalcogenides are the simplest and ideal ionic solids on which much experimental and theoretical work has been done in the past. They are model crystals for performing tests to validate new theories. They generally crystallize in either the NaCl or the CsCl structure. Various experimental and theoretical workers have extensively investigated their elastic dynamic and thermodynamic properties [8-62]. These solids undergo structural phase transition (B1-B2) at elevated pressures. A survey of the literature reveals that, although a large amount of experimental work has been done on the phase transition in alkaline earth chalcogenides, very scant attention has been paid to their theoretical understanding.

2. Phase transition

The homogeneous parts of any given assembly of atoms or molecules called phases are characterized by the thermodynamic properties like pressure, temperature volume and energy. A stable phase is always associated with minimum of free energy under specified thermodynamic conditions. If barriers do not exist, the state of the system becomes unstable and system moves into a stable or equilibrium state characterized by the lowest possible free energy. As the temperature, pressure or any other variable like an electric or magnetic field acting on a system is varied, the free energy of the system changes smoothly and continuously. Whenever such variations of the free energy are associated with changes in structural details of the phase (atomic or electronic configuration), a phase transformation (a phase transition) is said to occur. In this chapter, we are mainly concerned with the study of the high-pressure phase transition in the alkaline earth chalcogenides of rock salt structure. Phase transitions are associated with many changes in properties of the system at the macro and micro level. Consequently, below the transition temperature or pressure they acquire distinct properties such as spontaneous polarization, magnetization, nonlinearities in their electromagnetic behavior, etc. Several properties of the system sometimes attain large changes in their magnitude near T and P. These changes are normally known as anomalies. Anomalous change in elastic coefficients, dielectric constants, thermal expansion coefficients and specific heat is commonly observed [63].

All phase transitions are essentially due to the interplay of attractive forces between the particles of the system and their thermal motion. While attractive forces tend to hold them together and trap them in bound states, thermal energy leads to random and free motion. If enough thermal energy is not available, particles get trapped as in plasma-gas, gas-liquid and liquid-solid phase transitions. The reverse transitions occur when enough thermal energy is available [64,65].

2.1. Classification of phase transition 2.1.1. Thermodynamic classification of phase transition

The classical thermodynamics provides general and sound bases for the understanding of the phase transition in solids. A solid phase has a uniform structure and composition throughout and is separated from other phases by sharp boundaries [66]. At these boundaries, discontinuous changes occur in structure and/or composition. During the phase transition, whereas the free energy of the system remains continuous, thermodynamic quantities like entropy, volume, heat capacity and so on undergo discontinuous changes.

The classification of phase transition by Ehrenfest [67] depends on the relation between the thermodynamic quantity, which is undergoing discontinuity, and the Gibbs free energy function. According to this, a transition is said to be of the same order as the derivative of the Gibbs free energy, which shows a discontinuous change at the transition.

$$G = H - TS = U + PV - TS \tag{1}$$

$$dG = dU + PdV + VdP - TdS - SdT$$
 (2)

$$dG = VdP - SdT (3)$$

The first and second derivative of the free energy may be written as

$$\begin{split} &\left(\frac{\partial G}{\partial P}\right)_T = V; \\ &\left(\frac{\partial G}{\partial T}\right)_P = -S \\ &\left(\frac{\partial^2 G}{\partial P^2}\right)_T = \left(\frac{\partial V}{\partial P}\right)_T = V\beta \\ &\left(\frac{\partial^2 G}{\partial P \partial T}\right)_T = \left(\frac{\partial V}{\partial P}\right)_P = V\alpha \end{split}$$

$$\left(\frac{\partial^2 G}{\partial T^2}\right)_P = -\left(\frac{\partial S}{\partial T}\right)_P = -\frac{C_P}{T} \tag{4}$$

Here C_p , V, α and β are the heat capacity, volume, thermal expansivity and compressibility respectively. Thus the transformations in which a discontinuous change occurs in heat capacity, thermal expansivity and compressibility, belong to the second order.

Gibbs free energy given by Eq. 1 for different crystal structures can be written as

$$G_{B1}(R_1) = \phi_1(R_1) + 2PR_1^3$$

for NaCl (B1) phase

$$G_{B2}(R_2) = \phi_2(R_2) + \frac{8}{3\sqrt{3}}PR_2^3$$

for CsCl (B2) phase

$$G_{B3}(R_3) = \phi_3(R_3) + 3.08PR_3^3$$

for ZnS (B3) phase

At phase transition pressure P₁, G_{B1} (R₁) = G_{B2} (R₂) (for NaCl to CsCl transition) and G_{B3} (R₃) = G_{B1} (R₁) (for ZBS to NaCl transition). Here, the abbreviations Φ_1 Φ_2 and Φ_3 represents cohesive energies for B1, B2 and B3 phases respectively. Also, R₁, R₂ and R₃ are the nearest neighbor separations corresponding respectively to these phases.

2.1.2. Structural phase transitions

When a solid undergoes phase transition by absorbing thermal energy, the transferred phase will possess higher internal energy. In the high temperature phase, their bonding between neighboring atoms would be weaker than in the low temperature phase. This results in a change in the nature of the first nearest neighbors (primary coordinates) or the next nearest neighbors (secondary coordinates). Burger [68,69] has classified phase transitions on the basis of the structural changes involving primary or higher coordinates. He also related the potential barriers for the transition (or the transition speed) to structural changes. The transformations where there are changes in primary coordination will involve more drastic changes in energy as compared to those where only second or higher coordination changes. This can be easily visualized in the case of ionic crystals, where energies of the ionic bonds vary inversely with the interionic separation, while the energies of the Van der Waals interaction vary as the sixth power of such separations.

Bueger had defined transformations of the bond type, where two polymorphs differ greatly in nature of bonding; examples of this kind are polymorphs of tin (grey and white), carbon (diamond and graphite) and phosphorus (yellow and black). It is well recognized today that the knowledge of crystal chemistry in terms of atomic arrangements and bonding in crystals is essential for understanding the properties of solids. Thus, it can provide a basis for classification and prediction of the nature of phase transitions. In making such predictions, we take into account that thermal phase transition, which generally occurs from a structure of low symmetry (and high order). A positive volume change also accompanies the transition of the first order. This relates to the fact that the high temperature phase tends to have a greater openness structure and lower coordination while an application of pressure will facilitate a transition involving an increase in coordination (negative volume change).

Let us consider cubic AB-type compounds. The compounds can have NaCl, CsCl or ZnS structure with 6:6, 8:8 or 4:4 coordinations respectively, depending on their radius ratios. We can predict the following types of transitions in AB compounds:

1. NaCl structure Pressure CsCl structure

Examples: NaCl, KCl, RbCl, NaBr, KBr, monoxides and monosulfides of some metals.

2. CsCl structure Heat NaCl structure

Examples: CsCl, NH₄Cl, NH₄Br, etc.

3. ZnS structure Pressure NaCl structure

Examples: AgI, NH $_4$ F, II-VI, IV-VI and III-V semiconductors and their alloys.

4. NaCl structure Heat Wurtzite structure

Examples: MnS.

5. ZnS structure Heat B23 structure Examples: AgI.

6. NaCl structure Pressure B9 structure

Examples: AgCl.
7. CsCl structure distorted NaCl structure

Examples: RbNo₃.

In the simplest ionic crystal, it is possible to employ Born theory to predict the nature of the phase

transitions. According to the Born criteria of the rigid ion model [70,71], the relative stability can be accounted for in terms of the cation-anion radius ratio. For the radius ratios larger than 0.72, the CsCl structure is preferred and still lower values of the radius ratios favor the ZnS structure. The simplicity of the Born model tempted workers to modify it marginally and account for the phase stability. It is thus important to note that the Born model is based on two main assumptions:

- 1. lons are point like changes and
- 2. The interionic forces are central in character.

Both these assumptions cause serious difficulties when small energy differences between structures are to be evaluated. Also in many of the ionic solids, covalent contributions are not negligible and their presence seriously limits the validity of the Born model. Later on, a theory of covalency and iconicity in crystals has been developed by Philips [72,73], which explains a number of properties in ANB^{8-N} crystals satisfactorily.

The present three-body potential discussed above has been used to study the structural and elastic behavior of some ionic crystals. It is well known that the polymorphic phase transition is one of the most important phase transitions in solids is a crossdisciplinary subject of vital current interest. There exists a huge literature on this subject, which abounds both theoretical and experimental investigations of pressure induced phase transition in several systems of solids. In the present investigation, we are however, interested in the pressure induced polymorphic phase transition in ionic solids. The important ionic solids crystallize in the rocksalt, zinc blende or cesium chloride structures. It is experimentally known that the application of a suitable hydrostatic pressure to the crystals originally in the rocksalt (B1)/, zinc blende (B3) phase causes a structural phase change to a cesium chloride (B2)/ rocksalt (B1) phase. In order to understand them and other standing changes accompanying B1 to B2 transitions, it is necessary to study the thermodynamics, kinetics and structural aspects of the polymorphic phase transitions. The present section is devoted to such detailed description of these phenomena.

2.1.3. Pressure induced phase transitions

The pressure variation causes the overlap of the outer electron shells and this creates the transfer (or exchange) of charge, which in turn changes the properties of the material. Structural phase transition and changes in elastic behavior of the materials are the result. These observations are similar ones caused due to pressure variations and have resulted in a vital role for pressure in the study of properties of a number of

compounds, alloys, etc. The present study is on the structural phase transition and their elastic behavior due to the pressure on alkaline earth chalcogenides of RS structure.

The effect of high pressure influences many of the physical properties of solids. Bridgman studied the field of high-pressure physics broadly and exposed many unique phenomena [74,75]. In recent years, high pressure has made rapid advances both with respect to the limit of the pressure range available and to techniques [74-76]. The most effective results of high pressure are the phase transition phenomena. High-pressure polymorphism appears to be a rule rather than an exception. The less efficiently packed or lose a structure, the higher is the probability of a pressure induced phase change. Even closed packed structures such as face centered cubic (FCC) and hexagonal closed packed (HCP) exhibit phase transition under pressure accompanied with small volume changes.

From the theoretical point of view, different approaches have been developed to study the structural phase transition under pressure. These approaches include various methods from empirical methods to the first principle calculations. Due to the continuous modifications in theory and computational techniques the *ab-initio* band structure calculations have obtained the calculation at small structure energy differences between different phases. Therefore the successful estimation of pressure induced structural phase transition is promising. For studying the structural phase transition mechanism the molecular dynamic methods are also worth mentioning here

In the solid state, pressure is inclined to hold back the large scale diffusion of atoms. Since the repulsive forces between the neighbouring atoms increase during compression under pressure. Hence at higher pressures the structure, molecular shapes and orientations are gradually distorted. At this condition the structure is ready to undergo the phase transition with a little displacement of atoms. These displacements are generally reversible in nature for crystalline to amorphous transitions. These displacements maintain the atomic correspondence between the parent and the product phases maintaining symmetry relationship between them [77-82].

2.1.4. Reversible and irreversible phase transitions

A phase transition in which the system returns to its original phase, on withdrawal of the factor that causes the phase transition, is known as reversible phase transition. On the contrary, the transition is called irreversible. A prominent example of an irreversible phase transition is that of TiO₂ (Antase) to TiO₂ (Rutile) [83].

In this section we have presented the review of classification of phase transition based on the status of kinetics [84-87]. Earlier studies on classification of structural phase transition were based on the rate of change of transition and crystallographic changes. Ehrehfest classified phase transition phenomena on thermodynamic basis. This classification was based on change of derivative of Gibbs free energy which shows discontinuity at the transition pressure or temperature. Another classification by Heinish [84] is available based on kinetic, thermodynamic classification, thermochemical and structural considerations. Burger classified phase transitions on the basis of structural changes involving primary or higher order coordination [85]. He also discussed the disorder transformations

2.1.5. Incommensurate - commensurate phase transitions

Incommensurate-commensurate phase transitions are fundamentally different from the normal commensurate transitions. In commensurate phase, the system does not have any space symmetry, where as outside the temperature interval of this phase the structure is crystalline. However, this does not imply that an incommensurate phase is amorphous. In fact, it has an ordered structure with periodic distortion, which does not fit with any crystal periodicity [88].

Pynn [88] has suggested a model to conceive the difference between commensurate phase and incommensurate phases. A chain of equally spaced atoms with separation can be considered for its understanding. A sinusoidal displacement of wavelength $4a_0$, when modulated over the chain, results in a structure which can be described in terms of unit cell of dimension $4a_0$. However, it is not necessary for a lattice modulation to always have a periodicity that is a rational multiple of a_0 . Such a modulation over the chain of atoms results in a structure that obviously loses its translational symmetry.

This structure cannot be defined in terms of original lattice constants a_0 and is referred to be incommensurate. Incommensurate SPTs are thus characterized by an order/ disorder corresponding to a wave vector (q_i) that cannot be expressed as a rational fraction of a reciprocal lattice vector. Recently these transitions have been explained by soliton waves [89,90], where the dispersion curve splits into two branches known as amplitude with ordinary soft mode behavior and phase. They described phase distortion whose frequency vanishes at a zone point q_c (a rational fraction of reciprocal lattice vector) where incommensurate phase vanishes. Cowly and Bruce describe the phase diagram of such transitions [91].

3. Experimental techniques

With the continuous advancement in techniques of highpressure generation and measurements of properties of matter under pressure, the pressure range is increasing day-by-day. The effect of high pressure influences many of the physical properties of solids. Bridgman [92,93] carried out a broad study in the field of high-pressure physics and exposed many unique phenomena. These studies have provided understanding of many aspects of the solid state of matter. The synthesis under high pressure and temperature of industrially important material such as diamond and many other applications of high pressure in industry have added new dimensions to this field. Although the present study is mainly concerned with the theoretical interpretation of highpressure behavior of heavy alkaline earth chalcogenides compounds, it involves a direct comparison of the predictions with experimental theoretical It is therefore essential to understand the status of current experimental methods, their usefulness and technical limitations. In view of this fact, we have reported a brief description of the high-pressure techniques presently employed to study the pressure induced phase transitions and phonon properties of solids in this chapter.

High-pressure measurement techniques may be divided into two major categories, *viz.* static and dynamic. Amongst the dynamic methods, the shock wave methods are most commonly used in the laboratory for the study of high-pressure behavior of solids. Static methods are the piston cylinder (P.C.), the tungsten carbide (WC) and the diamond anvil cell (DAC).

3.1. Dynamic methods

Ultrasonic and shock wave methods are the dynamics methods, which are of interest for the study of high-pressure elastic behavior and phase transition of solids. A brief description of these methods is presented below.

3.1.1. Ultrasonic techniques

Research concerning the elastic properties of single crystals offers a direct means of obtaining useful information of the bonding relationships. Both ultrasonic and static compression methods are used to study the high-pressure elastic behavior. Ultrasonic methods have the advantage that it gives all the elastic constants of crystal and their variation with pressure more accurately then the bulk methods.

In this method, an ultrasonic pulse (10 to 20 MHz) is generated by a quartz piezoelectric transducer and

transmitted through the test crystal. The reflected pulse from the rear surface of the crystal reaches back to the transducer, makes successive reflections, and is detected each time. The actual physical measurement consists of the transit time by standard electronic instruments. For measurements of pressure effect, the small pressure induced changes in ultrasonic pulse transit time can be measured by an automatic-gated carrier pulse superposition equipment with a resolution of better than part in 107. The experimental details concerning the ultrasonic methods have been given in [94]. Velocities of the longitudinal and transverse waves propagated in the specific crystallographic directions are functions of the second order elastic constants or their combinations. Chang and Graham [95] have used this method to study elastic properties of some metal oxides in NaCl phase.

3.1.2. Shock wave techniques

Subjecting a sample to a shock wave produced by detonating explosives can generate pressures in the region of 500 GPa and above. Pressures of similar magnitude are also produced if a solid accelerated by the denotation of some explosive is made to impinge on the sample. In either case, the result is the introduction of a step pressure that propagates through the sample, and changes the shape as a result of the action of inertial forces derived from mechanical properties of the sample. This method produces dynamic pressures with a time duration that poses experimental problems requiring sophisticated instrumentation. The propagation of shock waves through solids is quite complicated, which leads to involved data reduction procedures.

In a special shock wave, the sample should be maintained in a state of uniaxial strain for sufficient time for measurements to be completed. This is achieved by different loading systems, which are designed to apply loads over large plane areas of samples. Some important loading systems are Contact Explosives, Flyer plates Techniques, and Projectile impact technique. Most of our knowledge about shock-induced effects is derived from measurements of shock and particle velocities produced by well-controlled loading. The shock wave techniques involve measurements of shock velocities determined by detecting times of arrival of the wave at two or more stations at a known location. In these experiments, arrival times are to be determined within a few nanoseconds to achieve suitable accuracy in the derived shock velocity. Resistivity measurements have been of limited value owing to the complications of the environment; these are serious limitations on the type of information that can be obtained by this technique. So, far attempts have been made mostly to obtain the

equation of state of solids from the experimental shock wave data. For these reasons, shock wave techniques do not enjoy the popularity of other high-pressure techniques even though the shock wave technique can produce extremely high pressures. The details of this technique can be found in [96].

3.2. Static methods

The static methods allow the measurement to be carried out under purely hydrostatic condition. Sufficient time to attain thermodynamic equilibrium under isothermal conditions is available for static measurements. Hence, the conditions assumed in the theoretical calculations are experimentally achieved in these methods. With the recent refinement in the diamond anvil cell technique, the range of pressure in static experiments has been increased up to ~550 GPa.

3.2.1 Piston cylinder methods

Bridgman carried out the earliest compressibility measurements utilizing the versatile, high-pressure piston cylinder (P.C.) [92,93]. The P.C. apparatus consists of laterally supported tungsten carbide by application of Arial load. A ram driven tungsten carbide (W C) piston pressurizes the specimen confined in the cylindrical chamber. While simple single stage pumps are adequate for generating pressures up to a few thousand atmospheres, higher pressures require some form of a pressure-multiplying device that may be called a press or an intensifier P.C. press (as shown in Fig. 1), which utilizes two hydraulic rams. The ram at the top of R1 carries the platen P1. The pressure vessel is clamped between the platens P1 and P2, by operating the ram R1 such that the tungsten carbide core supports the entire load. This is called end load. Forcing a tungsten carbide piston in to the pressure vessel pressurizes the sample placed in the pressure vessel; the ram R2 provides the necessary load. The design of the high-pressure equipment becomes more difficult as the working pressure is increased. The limiting working pressure is reached when the stress on the inner surface of the vessel exceeds the field strength of the vessel material. A non viscous fluid is used as a pressure transmitting medium up to 3 GPa and for higher pressures up to 10 GPa the sample is enclosed in a thin sheet of indium or some other soft material which will act like pseudo liquid to create approximately hydrostatic pressure [97].

3.2.2 Diamond Anvil Cell-Techniques

The study of materials at high pressure is experiencing great current activity because of recent refinements of the diamond–anvil cell technique. The phenomenal

advances [98,99] in the mechanical design of the diamond-anvil cell (DAC) have made better apparatuses for carrying out detailed study of condensed matter behavior under high pressure. Brilliant cut, gem quality diamond stones are generally used as anvils. The surface shapes of the stones are customized for the pressures at which the experiments have to be performed. The stone containing a reasonable concentration of evenly dispersed nitrogen platelet impurity (type I) is stronger, but has considerable absorption in the mid infrared region [100]. Purest diamond (type II) is needed if the diamond anvil is required to be transparent throughout the infrared region. The purest diamond does not sustain ultra high pressure, as it tends to cleave easily. For fabricating a DAC, the cut, color, clarity and carat are the four most important characteristics.

Color in diamond is due to the absorption band in the visible region arising as the consequence of the characteristic impurities (aluminum, nitrogen etc.). Near colorless, light brown or light yellow diamonds are acceptable from the point of view of strength. However, for spectroscopic experiments in the visible region, optically transparent diamond is essential. The clarity of the diamond is important for its use in optical spectroscopy. All stones for which the ratio of the intensities of the second order Raman peak to the fluorescence exceeds three are acceptable for optics experiments. An important feature that is crucial for achieving ultra high pressure is the shape of the diamond anvil. A perfectly circular culet (for pressure up to 60 GPa) or a beveled culet (for ultra high-pressure work) is the most desirable requirement. Trench fabrication in the conical surface, close to the culet, is expected to arrest the gasket material flow and hence to enhance the pressure sustaining capability of the diamond anvils (DAs).

It is observed that under loading, the pressure increase sharply from the culet edge to the culet center, where it maximizes. Above a certain pressure limit, a part of the applied load is used up in deforming the DAs. The simulation work indicates that under uniaxial stress, a mechanical instability sets in at $\Box 550$ GPa [101,102]. Under loading, once the deformation is initiated, the anvil in the central part starts cupping.

Further increase in the load increases the cupped area as well as the stress around the reaming part of the culet, which is an annulus. When this annulus area becomes small and is around the edge only, the DA fails due to chipping. The introduction of a bevel in the DA is an important landmark in enhancing the pressure sustaining capability of diamond anvils, since bevels postpone the cupping of the DA.

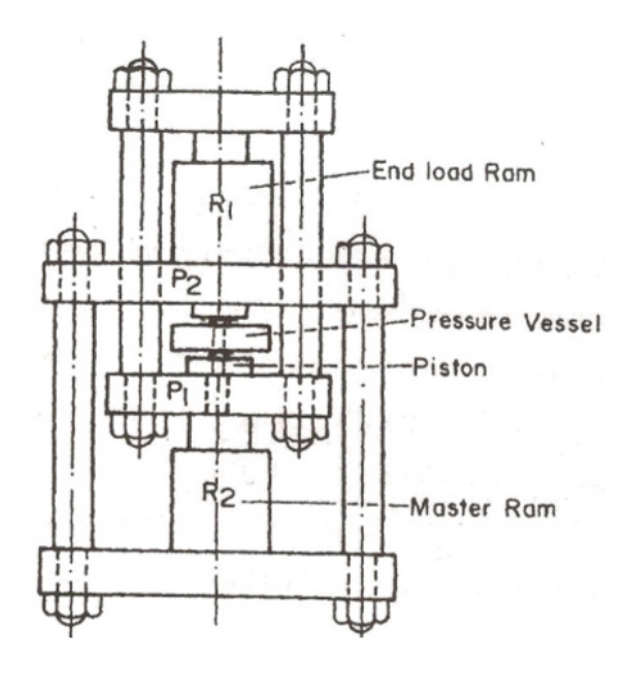


Figure 1. Piston-cylinder apparatus.

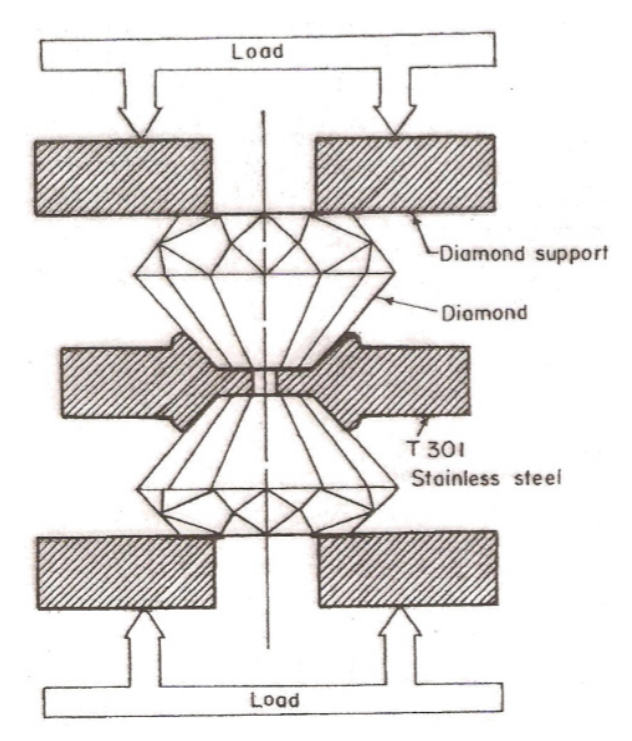


Figure 2. Opened diamond anvil cell configurations with a metal gasket for sample confinement in a pressure medium.

The basic principle of the DAC is depicted in Fig. 2 where a metal gasket is compressed between the culets of the DAs. The gasket has a central hole that is filled with pressure transmitting medium, the sample of the investigated specimen and the pressure calibrate, such as ruby chip. Since the area of the culet is very

small a modest load of □10⁴ N is sufficient to generate a pressure in excess of 100 GPa. For achieving success in DAC experiments, the gasket hole must be centered accurately with respect to the culet centers. Use of very high gasketing material is also important to avoid compressive yielding. Six major type of DAC are:

- 1. NBS Cell
- 2. Mao-Bell Cell
- 3. Hubber Syaseen Holzapfel Cell
- 4. Basset Takahashi Stook Cell
- 5. Lee Toullec-Pinceaux-Loubeyre Cell
- 6. Merril-Basset Cell

3.2.3. Cubic press

The cubic press has H. Tracy Hall's design and is of 200 tones. This equipment is capable of generating pressures up to about 60 kbar and temperatures of the order of 1500°C. The press has six tungsten carbide anvils, which move synchronously and press the sample in the form of a cube. A pair of opposite anvils also acts as leads for electric current to heat up the specimen. The schematic arrangement of anvils in the cubic press is shown in Fig. 3. The six anvils shown are advanced by six hydraulic rams towards the center of the cube [103].

For any high-pressure study, it is important to carry out pressure calibration of high-pressure equipment used. Conventionally, when one has to perform experiments at pressures higher than 2.0 GPa, well known pressure fixed phase transitions in Bi (I-II) at 2.54 GPa, TI (II-III) at 3.67GPA [104], Yb (fcc-bcc) at 4.0 GPa and Ba (I-II) at 5.5 GPa are used [103]. In this normal pressure calibration, the wires of Bi, Yb, TI, Ba, etc are surrounded by a sleeve of low shear strength material, typically made of AgCI. This minimizes the effect of pressure gradients. Non-hydrostatic stresses and deformation occur within the pyrophyllite, which is generally used as the solid pressure transmitting material.

Therefore, in order to have information about the behavior of the press in the range of 0 to 2.0 GPa, studies on the volume transitions in some inorganic materials such as KBr could be exploited [103]. In this recent work of the cubic press method, KBr has been found as one such material whose volume transition was studied as a function of applied load. Fig. 3 shows the reaction cell assembly used to study the volume transition in KBr. A sleeve was made with the above compound with a wire having a large pressure coefficient of resistance such as bismuth used at its axis. The resistance or the wire is measured as a function of applied load and the onset of transition is indicated by the discontinuity required to take up the volume change associated with the transition.

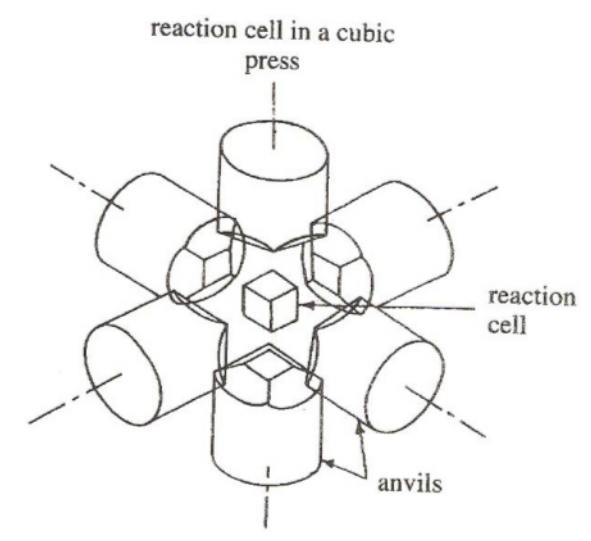


Figure 3. Cubic Press.

3.2.4. X-Ray diffraction

The DAC apparatus is utilized in most high-pressure X-Ray Diffraction studies. DAC coupled to X-Ray Diffraction can be used to study the crystal structure compressibility and pressure induced phase transition. X-Ray Diffraction experiments on powdered samples can be done either in energy dispersive or in angle dispersive mode [60,105,106]. Ultra high pressures and temperatures in a DAC are achieved at the expense of reducing the sample volume. The microprobe can be used for a variety of high-pressure experiments including single crystal XRD up to □50 GPa powder diffraction up to □300 GPa deviatoric strain measurements, and XRD at simultaneous high pressure and temperatures [107,108].

The X-Ray Diffraction (XRD) method with DAC is one of the popular experimental techniques for investigation of the materials under ultra high pressure. The low atomic number (Z) of diamond and small absorption co-efficient of it allow for the X-rays to pass through it. The basic instrumentations of different types of high pressure X-ray Diffractometers have been reported in earlier literature [109-111]. The X-Ray can be made incident on any region of the sample inside the DAC using the X-Ray Collimater. The X-Ray diffraction method can be broadly divided into two classes:

- 1. Single Crystal XRD, and
- 2. Powder XRD

Although single Crystal XRD method is ideally suited for structure determination, it is not suitable at very high pressures because the crystal breaks either due to structural phase transitions or due to non-hydrostatic stresses. The Single Crystal XRD techniques are restricted to 10-20 GPa [109,110,112,113]. Hence, Powder XRD methods are widely used at very high

pressures and it is an essential tool for many highpressure experiments. Applications of powder X-ray diffraction at high pressure include determination of symmetry, cell parameters, crystal structures, equation of states, elastic constants, phase transitions, rheology/ deformation, melting point, crystallinity and particle size powder X-ray diffraction can be further classified into two categories

- 1. Energy dispersive (EDXD)
- 2. Angle Dispersive (ADXD)

Both are based on Bragg's law:

$$2d_{hkl}Sin\theta_{hkl} = \frac{hc}{E_{hkl}} \quad \text{for EDXD}$$
 (5)

$$2d_{hkl}Sin\theta_{hkl} = \lambda_0 \quad \text{for ADXD}$$
 (6)

where h is Planks constant and c is the velocity of light. Gieessen and Gorden first introduced the EDXD technique in 1968 [113]. In EDXD, X-ray radiation is incident on the sample and the diffracted beam is collected at a fixed angle by using a solid-state detector. In this method, scattering angle is fixed during data collection. However, it can be changed to other angles if desired. Data acquisition time is short due to simultaneous acquisition of data at all energies and detector efficiency. Resolution in EDXD method is poor than that of ADXD method due to energy resolution of the detector.

4. Theoretical methods

We are discussing in this section the theoretical studies of structural phase transitions involves concepts of interatomic bonding their interaction and model calculations. Although today we do not require them for the theoretically study of phase transition pressure and structural details. But, their importance lies in their simplicity which yields the insight into the underlying physics.

It is simple to understand the performance of some structures under increasing pressure. When the pressure is increased the structure with lower coordination number tends to adopt the higher coordination number. The nuclear repulsion energy reduces due to larger packing fractions. This results in the closed packed structure for the formation of high pressures.

It is concluded that nearly free electron theory is applicable even to the valence bands of diamond as suggested by the early studies of electronic structure [114]. In pseudopotential approximations, the core electrons are removed and valence effects are taken into account. The strong ionic potential is replaced by a

weaker pseodoptoential that includes the ion and the core electrons. In the nearly free electron theory sometimes these pseudopotentials treated as a weak potential for sp-bonded materials. The empirical pseudopotential was developed in 1950s [115]. This approach has been developed for studying the electronic structure calculation. Further modifications are still continuing. In 1970s Heine and Weaire [116] have proposed that the energy difference and their contributions to the band structure energy are insufficient to account for the observed differences in phase stability.

Soma *et al.* [117] predicted the reasonable results for the coexistence pressures and volumes in II-IV and III-V group compounds. They included the term pair wise interatomic interaction potential in the pseudopotential perturbation theory. This pseudopotential explained the energy difference between the structures at a particular volume. Hence this potential is a rearrangement of potential for the atoms at constants volume. The trend in the crystal structure of sp-bonded elements, including a pressure- temperature phase diagram for the IV-A group elements have been well explained by Hafner and Heine [118] using the rearrangement potential.

4.1. First principle calculations

An accurate prediction of the total energy of a material as a function of atomic positions is possible by first principle electronic structure calculations [119,120].

4.1.1. Density-functional theory

In density functional theory (DFT) fundamental variable is the electronic charge density. Otherwise complicated body problems for the electron are simplified through DFT [121]. It is rigorous formulation of the many body problems. The total energy of ground state energy is a unique functional of charge density. If the density is Correct this functional is minimal. To study the electronic systems in terms of electronic density, the suitable theory is the variational principle of DFT. A poor agreement with experimental results is seen when Hohenberg -Kohn theorem is applied with the approximation of kinetic and exchange correlation energy functionals [122]. Conceptually, Hohenberg-Kohn theorem was at advanced level but could not properly do well at practical level. After this Kohn and Sham [123] tried to avoid approximation of combination from kinetic energy, but it was not easy to approximate an explicit functional of density. They conceptualize an auxiliary non-interacting system which can reproduce charge density of interacting system. Kohn-sham equations (non interacting Schrodinger like equations) are taken for ground state of non-interacting system and have been solved self consistently. The Kohn -Sham

equations are

$$\left[-\frac{1}{2}\nabla^{2} + V_{H}(r) + V_{XC}(r) + V_{ext}(r)\right]\varphi_{i}(r) = \varepsilon_{i}\varphi_{i}(r)$$
 (7)

Where V_H is the electronic potential from the electronic charge density, which is known as the Hartree-potential, V_{xc} is the exchange-correlation potential and V_{ext} is the external potential from the ions. The electronic density is given by

$$\rho(r) = \sum_{i=1}^{N} \left| \varphi_i(r) \right|^2$$

where the sum is over the N levels of lowest energy (N is the number of electrons in the system).

4.1.2 First-principles molecular dynamics

The first principle molecular dynamics method was a big achievement of Car and Parrinello in practical DFT calculations [124]. This work was a milestone in the sense that it opened the door for efficient algorithms and applications to new problems. In first principle molecular dynamics, classical approaches as well as first principle calculations are used. For the motion of atom classical Newton's law of motions are used and for the forces on atoms first principle methods are used. This way we achieve accuracy for describing bond breaking due to phase transition phenomena. The important part of this theory lies in the description of dynamical simulations. From first principle molecular dynamics we can get information about not only evolution of a phase transition but also the transition path along with relative orientation of phases. It is easy to find new stable phases of solids during cooling from high temperature using this theory. Melting of solids with P-T diagram can be easily studied with first principle molecular dynamics method [125]. Focher et al. [126] and Scandolo et al. [127] studied phase transition in Si and C using first principle molecular dynamics method. The first principle molecular dynamics method has some limitations as these simulations can run for tens of pico seconds which do not match with the requirement of some process. Also these computations cost a lot. Despite their limitations, these first principle molecular dynamics can have important role in future theoretical investigations of structural phase transition phenomenon.

4.2 Tight-binding theory

This theory is suitable for close packed systems. In tight binding theory the electronic state of a molecule may be written as a linear combination of atomic states of the atoms which constitute this molecule

$$|\psi_k> = \sum_i U_i |\psi_k> \tag{8}$$

Here $|\Psi_{\rm k}>$ is the electronic state of molecule and $|\Psi_{\rm k}>$ is the atomic state of atom. This may be simplified by taking only minimal basis of set of such atoms. Only those states from shells are taken which are partially occupied in the free atom. In most cases, the states are valance s and p-states suitable for row of position of atoms in periodic table. The minimisation of the expectation values of the Hamiltonian for the state $|\Psi_{\rm k}>$ with respect to the coefficients $U_{\rm i}$ provide us the electronic eigen states and eigen values $\epsilon_{\rm k}$. The atoms will be neutral, when these states are occupied by the number of electrons present and we have the sum of eigen values of the occupied states

$$E_{TOT} = \sum_{OCC} \varepsilon_k \tag{9}$$

may be taken as total energy of the system because when atoms are rearranged, the change in the energy of the compound will be equal to the change in the sum of eigen values. Since most of the properties of compounds may be written in terms of energy, this theory provides a vast range of properties of materials.

To further proceed, now we need tight binding parameters which come from Hamiltonian matrix on the basis of atomic states. The atomic term values E_{ij} as Hartee- Fock free atom term values are taken in these parameters. An example may be seen in table given in [128]. Apart from atomic term values the coupling between electronic states on neighboring atoms V_{ij} is also included. This nearest neighbour coupling can be taken as universal values as

$$V_{ss\sigma} = -1.32\hbar^2 / md^2$$
 $V_{pp\sigma} = 2.22\hbar^2 / md^2$ (10)
 $V_{sp\sigma} = 1.42\hbar^2 / md^2$ $V_{pp\pi} = -0.63\hbar^2 / md^2$

The subscripts ss and sp are angular momentum quantum number of atomic state and σ is the angular momentum of the two states around the internuclear axis.

Where do these couplings come from? The question has an interesting answer that also gives us some idea how much confidence we can have in them. Initially, these forms came from fitting an analytic form to values obtained from careful band calculations on semiconductors [129]. It was then realized that these forms followed from the fact that semiconductor band structures could be well described by tight-binding theory but at the same time were very free electron-like [130].

4.2.1. The neglect of coulomb effects

We now have all the needed parameters for studying the electronic structure, and therefore the properties,

of simple covalent (ordinarily semiconducting) and ionic solids. We should point out, however, what has turned out to be the most serious approximation given above: that is the assumption that each atom remains neutral in the solid. Frequently within the tight-binding context the atoms become charged - a sodium atom in rock salt is found to have a net charge near 0.8, and this must be taken into account to obtain reasonably accurate predictions of some properties. This has been undertaken, including self-consistent determination of the charges, and significantly improves agreement between theory and experiment [131]. The corrections are not so large as one might at first think since the shift in energy levels on one atom, due to its charge, tends to be cancelled (usually to within 10%) by the shift due to its neighboring atoms which have opposite charge.

4.3. AB-INITIO calculations

An extension to both molecular dynamics and electronic structure came as ab-initio molecular dynamics. Other known names of these methods are Car-Parrinello, Hellmann-Feynman first principle, quantum chemical, on-the-fly, direct, potential free, quantum, etc. molecular dynamics. In all these ab-initio molecular dynamic methods forces acting on the nuclei are computed from electronic structure calculations. The electronic variables are taken as active degrees of freedom in these calculations. So any complex system can be studied using molecular dynamics, if a suitable approximation solution is provided for the many body problems. This means selection is shifted from model potential to particular approximation for solving the Schrodinger equation [132]. A system is evolved following the basic laws of physics without the experimental input in the form of ab-initio molecular dynamics and so was named 'Virtual Matter Laboratory' [132] with vast applicability.

4.4. GWA approximation

In Kohn-Sham equations [133] eigen values are taken as single particle energies and compared with photoemission spectra but many times this led to incorrect predictions. Taking quasi particle concept [134] was the correct way for the interpretation of photoemission spectra. First time gradient wave approximation (GWA) was applied by Hybersten and Louie [135] to real compounds. Godly et al. [136] then successfully repeated similar results with using same approach. Applying gradient wave approximation (GWA) to rare earth compounds was not possible as there was complexity in calculating the self energy. Schilfgaarde et al. [137] applied quasi particle self consistent GW (QSGW) calculation to Gd, GdP and GdAs and resulted in overestimation of the position of the minority Gd f shell by 4 ev, Lembrecht

[138] predicted GdN as a narrow indirect gap insulator using linear muffin tin orbital method taking quasi particle energy gap corrections scale inversely with the dielectric constants. They reported that alignment of Gd 4f magnetic moments may result in tuned band gaps.

4.5. Dynamical Mean – Field Theory (DMFT)

Modernization and advancement in theoretical techniques resulted in a successful method called dynamical mean field theory (DMFT) suitable for the study of strongly correlated compounds with local Coulomb interaction [139]. This theory was based on local impurity self consistent approximation [140] originally based on many body problem of Weiss mean field theory [141]. The dynamical mean field theory takes many degrees of freedom to solve lattice problem and it is exact in the limit of high lattice coordination numbers [140]. One of the methods for solving Anderson impurity model is Monte Carlo interactive perturbation method. Now the DMFT can be clubbed with other electronic calculations like LDA+DMFT [142] or can be used separately [143,144]. Several Mott insulators have been successfully studied by DMFT. Other examples of this success are transition in cerium and the d phase of plutonium.

4.6. Model calculations

The necessity of charge transfer mechanism has been pointed out by a number of physicists [145-161]. They have concluded that results of two body potential models can be further improved by including the charge transfer mechanism in the potential model. This mechanism owes their origin due to the non-orthogonality of the electron wave function. This model has successfully described the static, dynamic dielectric, optic, anharmonic, elastic and phase transition properties of various solids. It is due to long range three body interactions that are required to describe Cauchy-violations. Also, it explains a comprehensive and unified description of lattice static and dynamic properties of semiconductors, molecular and ionic materials with their different structures. The study of the dynamics of atoms in crystal is essentially a many body problem and the solutions of the Schrodinger's equation become difficult due to describing the interaction mechanism and the crystal properties that arise. The ionic solids are well known to be model materials, which have been the ideal vehicle for testing the accuracies of interionic interaction. The exact knowledge of these potentials is also essential for the prediction of most of the properties such as the specific heat, thermal expansion, thermal conductivity, phase transition and dielectric properties of crystal.

Phase transition phenomena studies in ionic compounds using modified interaction potential model

(MIPM) found to be successful in variety of compounds [8-62]. This model includes long range coulombic, three body interactions van der Waal and short range overlap repulsive interaction possible corrections are made to include covalence for partially covalent compounds correctly [163,165-169]. This covalency effect becomes even more important under pressure when interionic separation reduces and ions overlap.

Another improvement to the model included zero point energy effects, which are the lowest possible energy that the compound may posses and is the ground state energy of the compound. This term shows a small effect in Gibbs's free energy but cannot be ignored completely. This modified model has shown a reasonable study of a number of the present group of compounds [162-169].

5. Results for each materials

In this section, we review phase transition pressure, volume collapse, elastic constants and bulk modulus of alkaline earth chalcogenides on the knowledge of present, and others theoretical and experimental data. For the systematic analysis of these alkaline earth chalcogenides, we have arranged them in five groups as barium chalcogenides, strontium chalcogenides, calcium chacogenides, magnesium chalcogenides and divalent metal oxides in the different sub sections. A review of the information pertaining to the phase transition pressures and volume collapses are summarized in Table 1. An assortment of experimental and theoretical data of phase transition pressure and value collapse is reviewed. The important ionic solids are well known to crystallize either in the rock salt (B1) structure with face centered cubic space lattice or in the cesium chloride (B2) structure with simple cubic space lattice, under high pressure. The majority of alkaline earth chalcogenides crystallize in NaCl structure at normal condition. At elevated pressures, the materials undergo structural phase transition associated with a sudden change in the arrangement of the atoms. The atoms are rearranged in new positions leading to a new structure. Experimentally, one usually studies the relative volume changes associated with the compressions. The discontinuity in volume at the transition pressure is obtained from the phase diagram.

5.1. SrX

The strontium chalcogenides SrS, SrSe and SrTe are found in six fold coordinated NaCl-type (B1) with space group *fm3m* structure. Under pressure they show a phase transition to CsCl-type (B2) with space group *Pm3m* structure at 18, 14 and 12 GPa [9-13]. This transition is

associated with a sudden collapse in volume showing the occurrence of first order phase transformation. The parent phase is face centred cubic (NaCl) having six atoms of opposite type, while the product phase CsCl here is body centred having eight atoms of opposite type. Hence in this transition, coordination number increases from six to eight. On further increasing pressure chalcogenides transform to metallic phase [9]. Comparing to other chalcogenides, less theoretical studies are available for SrX compounds

The pressure induced structural phase transitions and associated volume changes in CaTe and SrTe have been investigated by Zimmer *et al.* [14] using X-ray diffraction. They reported (B1-B2) transition in SrTe at 12 GPa. Luo *et al.* [17] reported (B1-B2) transition in SrSe at 14.2 GPa with volume reduction of 10.7% by X-ray diffraction using synchrotron source.

Recently Khenata *et al.* [9] have studied SrS, SrSe and SrTe in B1 and B2 structures and reported transition and metallization pressures. These compounds show a decrease in band gaps under pressure and it results in drop of d type conduction band in energy below the top of the filled P-type valence bands. The fundamental optical absorption of SrX chalcogenides was measured by Saum *et al.* [12] in the energy range 2.5-5.8 ev. In case of SrTe Zimmer *et al.* [14] reported the optical reflection and absorption spectra in the pressure range 0-40 GPa at 300 K.

Further recent studies are available on transition phenomena and related properties using density functional theory (DFT) calculation [18,19]. A B1 (NaCl structure) to B2 (CsCl structure) and related properties of SrS have been investigated by *ab-initio* plane wave pseudopotential density functional theory and quasi harmonic Debye model [18]. The structural stabilities and electronic properties of SrX (X=S,Se,Te) under pressure have been investigated using first principle calculation based on density functional theory (DFT) with plane wave basis. Jha *et al.* [150] investigated a B1-B2 transition under pressure in BaSe, BaTe and SrTe using a three body potential. But, they ignored the van der Waal interaction and covalency effect.

5.2. Barium chalcogenides

Alkaline earth chalcogenides (AY: A=Be, Mg, Ca, Sr, Ba; Y=O, S, Se, Te) are large gap insulators with closed shell ionic system. They crystallize in NaCl-type (B1) structure at ambient condition. Their behaviour under pressure and metallization phenomena have attracted attention of many researchers [8,15,24,25] to study them through advanced high pressure techniques.

Barium chalcogenides (BaX) belonging to the family of alkaline earth chalcogenides under high pressure

show a first order phase transition from B1 (NaCl-type) to B2 (CsCl-type) structure at 6.6, 6.0 and 4.8 GPa respectively [8,15,24,25]. Further increasing pressure, metallization results in the CsCl structure. These closed shell insulating compounds show a decrease in band gaps on further increasing pressure. Finally there is a dropping of d-type conduction band in energy below the top of filled p-type valence bands.

First-principles calculations have been used to investigate the elastic and the bonding properties of barium chalcogenides BaS, BaSe, and BaTe at equilibrium as well as high pressures using full potential-linearized augmented plane wave (FP-LAPW) method within density functional theory (DFT). A numerical first-principles calculation of the elastic constants was used to calculate $\rm C_{11}$, $\rm C_{12}$, and $\rm C_{44}$ for these compounds. Additionally, the nature of the chemical bond in these compounds was analyzed. F. El Haj Hassan *et al.* [151] investigated the bonding character of BaS, BaSe, and BaTe in terms of electronic charge density and found out that the strong charge localization around the anion side let these compounds behave as the most ionic ones among the alkaline-earth chalcogenides family.

Although the structural and electronic properties of BaX compounds have been investigated, both experimentally [8,15,24,25,152,153] and theoretically [154-160] during the past few years, the elastic and bonding properties of these compounds have been less studied. To the best of our knowledge, there are no experimental or theoretical works exploring the iconicity factor of BaX compounds, and no experimental values of the elastic constants have appeared in the literature.

5.3. Calcium chalcogenides

Among the AX compounds Ca-chalcogenides seem to be more challenging as they have high cation and anion radius ratio resulting in high phase transition pressures. The high pressure structural studies of these chalcogenides have been performed experimentally using the x-ray diffraction (XRD) technique to reveal the first-order phase transition from the NaCl (B1) to CsCl (B2) phase [17] at pressures 40, 38 and 33 GPa in CaS, CaSe and CaTe, respectively. This XRD technique has also been used to observe the phase transition (P,) and Pressure-Volume (PV) relationships in CaTe (P, = 35 GPa) and SrTe (P, = 12 GPa) [14] which have the smallest cation and anion radius ratio [161] among the AX chalcogenides. The phase transition pressure has also been observed [30,8,15,23,25] to be in between 33-35 GPa in CaTe. The transition pressures of calcium chalcogenides are although higher than SrX, SmX, EuX and BaX, but the volume collapses at the transition pressure in CaSe (8%) and CaTe (4%) are comparatively

Table 1. Lattice constants a_0 (Å), bulk modulus B (GPa) and pressure derivative of bulk modulus B' of B1 and B2 phases for present chalcogenides.

Solid		$\mathbf{a}_{_{0}}$	(Å)			_	GPa)				B'	
	Expt.	B1 Theory	Expt.	B2 Theory	Expt.	31 Theory	Expt.	B2 Theory	Expt.	B1 Theory	Expt.	B2 Theory
SrS	6.024ª	6.076 ^b	3.61ª	3.68 ^b	58ª	47 ^b	68.38 ^f	50.0 ^b	-	4.19 ^b	-	3.88 ^b
		5.776°		3.481°		62°		67.3°		4.3°		4.2°
						54 ^d		71.6 ^f 68.00 ^g		4.34 ^f		4.33 ^f
						58.6° 51.9 ^h		49.43 ^h		4.3° 4.01 ^h		4.2° 3.75 ^h
						51.53 ^h		49.40 ^h		3.98 ^h		3.69 ^h
SrSe	6.236 ⁱ	6.323 ^b	3.77 ⁱ	3.838 ^b	45 ⁱ	41 ^b	46 ⁱ	43 ^b	4.5 ⁱ	3.76 ^b	4.5 ⁱ	3.88 ^b
		6.026°		3.633°		52°	51.54 ^f	59°		4.5°		4.2°
						46 ^d		55.731		4.35f		4.09f
						50.3°		53.8°		4.5°		4.5 ^e
						45.2i		46.5 ⁱ		5.12 ^h		5.27 ^h
						47.66 ^h		42.48 ^h		5.00 ^h		5.09 ^h
						47.31 ^h		42.27 ^h				
SrTe	6.66	6.76 ^b	3.99	4.123b	39.5 ^j	36 ^b	-	35 ^b	5.0 ^j	3.23 ^b	-	3.56 ^b
		6.48°		3.95°		44°		45°		4.2⁰		4.2e
						48 ^d		42.9e		5.44 ^h		5.68 ^h
						39.7°		32.7 ^h		5.31 ^h		5.51 ^h
						39.5 ^j		32.56 ^h				
						35.76 ^h						
						35.64 ^h						
BaS	6.389 ^k	6.270 ⁱ	-	3.730 ⁱ	39.42 ^k	50.86 ¹	34.02 ^k	56.74	-	4.76 ¹	-	4.79
		6.316 ^m		3.874 ^m		53.32 ^m		49.50 ^m		4.90 ^m		4.48 ^m
		6.469 ^m		3.850 ^m		42.36 ^m		45.25 ^m		5.81 ^m		4.38 ^m
		6.27 ⁿ 6.46 ^a		3.76 ⁿ		52.39 ⁿ		57.27°		4.92 ⁿ		4.24 ⁿ
		6.455°		3.85ª		40.25ª		43.60°		4.16a		4.16a
		6.196°		3.852°		51.9°		57.0°		4.3°		4.3°
		7.17 ^p		3.706°		52.46°		60.84°		4.16°		4.12°
	0.500	0.404		4.41p	40.4.000	40.05		54.991		3.87		2.37
BaSe	6.59 ^q	6.484 ¹ 6.511 ^m	-	3.870 ^l 3.874 ^m	43.4±2.6 ^q	46.25 ¹ 45.95 ^m	41.9±1.4 ^q	48.62 ¹ 49.50 ^m	-	5.39 ¹ 4.42 ^m	-	4.29 ^l 4.48 ^m
		6.696 ^m		4.000 ^m		36.36 ^m		49.50 ^m 39.42 ^m		4.42 ^m		4.46 ^m
		6.45 ⁿ		4.000 3.840 ⁿ		38.98°		59.42 59.82°		4.72 4.06 ⁿ		3.90°
		0.40		0.040		44.9°		49.5°		6.56°		4.4°
						38.2°		41.9°		4.5°		2.74
						46.8		55.96 ^f		4.11		, .
ВаТе	6.99 ^q	6.868l ¹	-	4.117 ¹	29.4 ^q	35.41	27.5 ^q	39.51	-	4.74	_	4.20
		6.920 ^m		4.122m		35.68 ^m		40.04 ^m		4.51 ^m		4.11 ^m
		7.121 ^m		4.263m		28.70 ^m		31.81 ^m		5.42 ^m		4.26 ^m
		6.87 ⁿ		4.080 ⁿ		38.96 ⁿ		48.44 ⁿ		3.63 ⁿ		4.52 ⁿ
		6.60 ^r				37.43 ^r		43.99 ^r		4.28 ^r		3.97 ^r
		6.63 ^r				36.78 ^r		45.52 ^r		4.27 ^r		4.02 ^r
		7.06 ^r				31.82 ^r		40.5 ^r		4.4 ^r		4.3 ^r
						36.3°		27.5°		4.5-5.4°		2.52 ^f
						28.8°		39.4°		3.97		
								41.15 ^f				
CaS	5.689 ⁱ	5.714°	3.46	3.4878	64.0 ⁱ	57.7°	64.0 ⁱ	59.9°	4.2 ⁱ	4.2-4.9e	4.2i	4.2e
		5.717 ^t		3.494 ^t		57.4 ^t		60.7 ^t		4.2 ⁱ		4.2i
		5.685 ^u 5.598 ^v		3.519 ^u 3.410 ^v		67.4 ^u 65.2 ^v		77.83 ^u 71.2 ^v		4.24 ^u 4.2 ^v		4.23 ^u 4.2 ^v
		0.000		0.410		64.85		67.4 ^f		4.2 ¹		4.2°
CaSe	5.916	5.920°	3.61 ⁱ	3.620°	51.0 ⁱ	48.56°	51.0 ⁱ	53.91°	4.2 ⁱ	4.1	4.2i	4.0
J436	0.010	5.968 ^t	0.01	3.653 ^t	51.0	48.75 ^t	31.0	51.41 ^t	7.2	4.1	T. C	4.2
		5.753w		3.532w		62.34 ^w		64.49 u		3.34×		4.12×
		5.851 ^u		3.621 ^u		63.94 ^u		58.29		4.39 ^u		4.26 ^u
		5.829 ^v		3.560 ^v		56.2 ^v 57.1 ^e		61 ^v		4.1 ^v		4.2 ^v
				3.658						4.1€		4.2e
СаТе	6.348 ⁱ	6.394°	3.93 ⁱ	3.917°	41.8 ⁱ	39.22°	41.8 ⁱ	40.14°	4.3 ⁱ	4.0e	4.3 ⁱ	4.1⁰
		6.396°		3.930°	42	39.60°		38.78°	5.0	4.308×		3.32×
		6.414×		3.940 ^x		43.26×		42.6×		4.36 ^u		4.2 ^u
		6.155°		3.796°		46.95°		47.3°		4.2		4.2 ⁱ
		6.255 ^u		3.847 ^u		45.2 ^u		58.18 ^u				
		6.231 ^v		3.780 ^v		42 ^v		50.2 ^v				
MgSe	5.463 ^y	5.503 ^z	-	3.4359 ^z	-	65.4 ^z	-	62.5 ^z	-	4.14 ^z	-	4.10 ^z
		5.4340 ^y		6.906 ^y		68.0 ^y		53.22 ^y		4.04 ^y		

Table 1. Lattice constants a_0 (Å), bulk modulus B (GPa) and pressure derivative of bulk modulus B' of B1 and B2 phases for present chalcogenides.

Solid		a	(Å)			В (С	aPa)				B'	
		B1		B2	ı	31	E	32		B1		B2
	Expt.	Theory	Expt.	Theory	Expt.	Theory	Expt.	Theory	Expt.	Theory	Expt.	Theory
MgTe	-	5.9242 ^z 5.8548 ^z 5.8460 ^z	-	3.6826 ^z	-	54.5 ^z 48.6 ^z	-	49.5 ^z	-	4.04 ^z 3.88 ^z	-	4.20²
SrO	5.16ª	5.073 ^b ′ 5.160°′ 5.197 ^{e′} 5.072 ^{f′}	-	3.049 ^b	91ª' 90.6 ^{d'}	105 ^{b'} 86 ^{e'} 96 ^{f'} 106 ^e 96 ^{g'}	-	115.3 ^b 116° 130 ^g	4.3ª	5.0b° 4.47e° 4.5e 4.49°	-	4.72 ^{b'} 4.1 ^e 4.4 ^{g'}
ВаО	7.023 ^{h'}	7.149 ^h 6.894 ^k			75.6 [†]	71.22 ^{h'} 66.33 ^{k'} 73 ^{r'} , 91 ^{r'} 73 ^{m'} 68 ^{m'} 86 ^{m'} 70 ^{m'}	-	74.69 ^h	5.67 [†]	4.52 ^{h'} 4.55 ^{k'} 1.51 ^{l'} 4.17 ^{m'}	-	4.07h'
CaO	4.81 ⁿ	4.72° 4.71° 4.8104° 4.714° 4.84 4.838	-	2.855 ^h	110 ⁿ ' 116.1 ^r	128h' 117f' 134f' 129o' 130o 111p' 125q' 102k' 122o'	-	138 ^h 130 ^p , 144 ^q , 122.1 ^k , 133.8°	4.26 ^{n'}	4.11 ^{h'} 4.3 ^{r'} 4.47° 4.2° 3.6° 4.3 ^{k'} 4.5°	-	4.2° 4.37° 3.5° 4.0° 4.3° 4.3°
MgO	4.21s' 4.20' 4.21u'	4.165h' 4.213° 4.259e' 4.162w' 4.25x' 4.20y' 4.167°' 4.214z'	-	2.604° 2.604° 2.6° 2.572°	160° 156°	171.0° 167.6° 160.0° 185.9° 159.7° 1869 172° 157z	-	163 ^h 170 ^w 193 ^y	4.15° 4.7°	4.29 ^h 4.01 ^e 3.40 ^w 4.26 ^x 4.09 ^e 3.53 ^y	-	3.39 ^h ' 3.54 ^{w'} 2.94 ^{y'}

* [152], * [22], * [86], * [173], * [176], * [172], * [171], * [167], * [171], * [144], * [174], * [170], * [170], * [175], * [177], * [177], * [178], * [179], * [35], * [180], * [181], * [182], * [183], * [183], * [9], * [43], * [171], * [184], * [185], * [186], * [186], * [187], * [187], * [187], * [187], * [188], * [188], * [188], * [188], * [189], * [189], * [188],

smaller than those obtained in these compounds. The significantly small volume collapse in CaSe and CaTe has been ascribed to the large disparity in their ionic radii among the heavy alkaline earth chalcogenides and hence the repulsive force between the large ions (anions) resist volume collapse at the phase transition in CaSe and CaTe as remarked by Luo *et al.* [17].

In order to reveal the interesting features exhibited by the high pressure phase transition and Pressure-Volume relations in CaX compounds, several efforts have been devoted using the full potential linearized APW [35], *ab initio* [36], pseudopotential [37,38] and tight binding [26] theories.

5.4. Magnesium chalcogenides

Wide band gap II-IV semiconductors present a large interest for visible light emitters in the blue green spectrum [53]. Compared to Mg based semiconductors column IIB compounds are very different in the electronic and bonding properties. This difference was attributed to the existence of a metal d band inside the main valence band in column-IIB compound semiconductors. The role of d

states in II-IV semiconductors was well studied [54]. The imperfect d orbital screening in group II-B compounds makes their atomic sizes and lattice parameters smaller than those for group II-A compounds. The absence of a d orbital in the Mg element results in increasing the band gap [55].

With a wide band gap (the band gap certainly exceeds 4.5 eV at room temperature), magnesium sulfide is one of the most promising semiconducting materials and least studied members of this family. Magnesium sulfide crystallizes in the rock salt structure, in which form it is a proposed component of interstellar dust [56]. Recently several groups have been able to produce magnesium sulfide (MgS) in zinc blende structure on GaAs either by metallo-organic vapor phase epitaxy or by molecular beam epitaxy [57-60].

In the case of magnesium chalcogenides, MgS, MgSe and MgTe are wide band gap semiconductors and are of technological and scientific interest. The first three have the rock salt structure and transform under pressure to the cesium chloride structure [61]. The last, MgTe, was first determined to have the wurtzite

structure [62], but recently it has been found that the wurtzite structure undergoes a phase transformation at 1-3.5 GPa to the nickel arsenide structure and that this structure persists after unloading and annealing [63]. The two *ab initio* calculations on MgTe are reported in the literature [64]. A nickel arsenide ground state (at T=0) was also found. For MgSe, one calculation of three structures was reported [65].

5.5. Divalent metal oxides

In this group of AX, the four divalent metal oxides (BaO, SrO, CaO and MgO) form an important group of alkali halides, as they are a link between highly ionic halides and largely covalent III-V compound semiconductors [51,52]. These compounds being the prime constituents of earth's lower mantle [53] have importance in geophysical and academic areas. These oxides are used in the development of lasers after doping with transition elements [54]. Many of the oxide phases found in earth's mantle undergo pressure dependent phase transformation within the first few kilometres of depth of earth. Such type of transformations and understanding of their effects are important from the seismological point of view [55].

Developing accurate theoretical models to describe the behaviours of ionic crystals specially that of oxides under high pressure is tedious job. The reason behind this is that these oxides show transitions at very high pressures which are accessible experimentally only by shock wave method. These methods provide data which neither correspond to adiabatic nor to isothermal compression. Earlier studies on prediction of phase transition pressure of MgO are available. Phase transition pressure as high as 500 GPa had been predicted by Mehl et al. [56] using a general potential linear augmented plane wave (LAPW) method. Effort by Bukowinski [57] using a total energy muffin tin APW program resulted in the prediction of (B1-B2) phase transition pressure at 200GPa. Hamely et al. [58] used electron gas potential and carried out a quasi harmonic calculation and calculated total energy in B1 phase of MgO. On the other side the experimental studies based on dynamic method shock wave [59] as well as static method diamond cell [60] method measured transition pressure of MgO for (B1-B2) transition to occur beyond 120 and 95 GPa respectively. These differences and contradictions between theoretical and experimental studies are found in MgO as well as in other oxides also. To cite instance, the transition pressure of SrO is predicted near to 200 GPa while experimentally measured data is 36 GPa. Jeanloz et al. [62] also found difference in experimental and theoretical results up to some extent. These differences and contradiction in results compel us to go for further refinements of theoretical techniques available eliminating deviations.

The results of MEG calculations could be improved by including many body interactions as suggested by Cohen and Gorden [44]. Neglect of many-body interactions also led to violation of Cauchy relations ($C_{12} \neq C_{44}$) which are quite significant in divalent metal oxides (DMOs). Also non additive three body interactions are found to be significant in DMOs as under high pressure in compressed conditions nearest neighbour distances decrease [81,82]. So for developing a realistic potential model for DMOs it is necessary to include three body potential [83,84] and van der Waal interactions for better matching with experiments.

Here Phase transition pressures, volume collapses and elastic properties results of the oxides of Ba, Sr, Ca, and Mg are presented. All these oxides are important materials to study. CaO is used for fuel gas treatment, drinking water softer, steel manufacturing and for the construction work. CaO shows a B1-B2 transition at around 60 GPa. The range of phase transition in MgO and BaO are higher while for SrO is lower than this. CaO has a well-characterized B1-B2 phase transition, reported to occur at around 60 GPa.

6. General discussion and conclusion

We have reviewed the present status of theoretical calculations on the high-pressure phase transition and allied properties of group II-IV alkaline earth chalcogenide compounds and evaluated the results with the experimental data. We have summarized a variety of theoretical and experimental results for lattice constants, bulk modulus and pressure derivatives of bulk modulus in B1 and B2 phases respectively for the present group of chalcogenides. This comparison of barium, strontium, calcium and magnesium chalcogenides has been presented in Table 1. It is clear from the table that the values of a₀, B and B₀ show in general the same behaviour of experimental and theoretical results [170-202]. In some cases, the theoretical values of these calculations overestimate the experimental results while in some cases these values underestimate the experimental results. The values of a₀, B and B₀ are not available for MgS for B1 and B2 phases. This compound is found most probable in B3 (ZnS) structure. Various experimental and theoretical calculations are available for MgO and CaO, BaS, BaSe and BaTe. The values of phase transition pressures and volume collapses,

 Table 2. Phase transition pressure and volume collapse.

Solid	Reference	Phase Transition Pressure (GPa)	Volume Collapse %
SrS	Experimental [17]	18	11.4
	Syassen et al. 1985 [152]	18	-
	Banu et al. 1998 [86]	17.1	11.1
	Khenata et al. 2003 [22]	18	11.0
	Xiao-Cui et al. 2008 [19]	18.17	10.8
	Cheng et al. 2008 [18]	17.9	-
	Varshney et al. 2008 [160]	17.5	7.5
	Kholiya et al. 2011 [172]	18.3	-
	Potzel <i>et al.</i> (2011) [176]	16.7	_
	Bhardwaj et al. 2009 [167]	18.6	10.18
2.50			
SrSe	Experimental [17]	14	10.7
	Banu <i>et al.</i> 1998 [86]	13.5	-
	Khenata et al. 2003 [22]	14.5	8.6
	Xiao-Cui et al. 2008 [19]	15.87	9.96
	Varshney et al. 2008 [160]	14.5	9.2
	Kholiya et al. 2011 [172]	13.9	-
	Potzel et al. 2011 [176]	16.2	-
	Bhardwaj et al. 2009 [167]	13.3	9.73
irTe	Experimental [17]	12	11.1
- 10	Zimmer et al. 1985 [14]	12	-
			- -
	Banu et al. 1998 [86]	11.2	
	Khenata et al. 2003 [22]	10.3	7.3
	Xiao-Cui et al. 2008 [19]	13.24	8.92
	Varshney et al. 2008 [160]	12.5	8.3
	Kholiya et al. 2011 [172]	11.9	-
	Potzel et al. 2011 [176]	14.1	-
	Bhardwaj et al. 2009 [167]	11.2	10.17
aS	Experimental [14]	6.5	16.7
	Yamaoka <i>et al.</i> 1980 [15]	6.5	13.7
	Kalpana et al. 1994 [155]	6.025	-
	Rhenata et al. 2006 [9]	7.3	
	Hassan <i>et al.</i> 2006 [151]	7.7	
		7.7	- 11.5
	Benamrani et al. 2010 (GGA) [146]		
	Benamrani et al. 2010 (LDA) [146]	4.75	7.4
	Kholiya et al. 2011 [172]	6.60	-
	Potzel et al. 2011 [176]	5.13	<u>-</u>
	Baohemadau et al. 2006 [170]	6.51	11.0
	Bhardwaj et al. 2008 [166]	6.9	11.76
aSe	Experimental [14]	6.0	11.14
	Grzybowsky et al. 1983 [24]	6.0	11.7
	Grzybowsky et al. 1984 [25]	6.2	5.0
	Weir <i>et al.</i> 1987 [153]	5.6	11.14
	Majewski et al. 1987	12.6	19.0
	Rao et al. 1991 [13]	8.5	-
	Hassan <i>et al.</i> 2006 [151]	6.8	-
			12.1
	Benamrani et al. 2010 (GGA) [146]	6.37	
	Benamrani <i>et al.</i> 2010 (LDA) [146]	4.41	7.4
	Kholiya et al. 2011 [172]	6.20	-
	Potzel et al. 2011 [176]	5.05	-
	Baohemadau <i>et al.</i> 2006 [170]	6.02	12.0
	Bhardwaj et al. 2008 [166]	5.4	12.20
ате	Experimental [14]	5.5	11.14
	Benamrani et al. 2010 (GGA) [146]	4.75	11.69
	Benamrani et al. 2010 (LDA) [146]	3.63	8.01
	Kholiya et al. 2011 [172]	4.50	-
	Potzel <i>et al.</i> 2011 [176]	4.16	<u>-</u>
	Baohemadau et al. 2006 [170]	4.50	12.0
	Bhardwaj <i>et al.</i> 2008 [166]	5.0	10.24
CaS	Experimental [17]	40	10.2
	Cortona et al. 1998 [37]	45	7.7
	Charifi et al. 2005 [35]	35.4-37.2	-
	Varshney et al. 2009 [160]	40	4.5
	Hao et al. 2010 [180]	40	-
	Potzel et al. 2011 [176]	39.3	-
		55.5	

Table 2. Phase transition pressure and volume collapse.

Solid	Reference	Phase Transition Pressure (GPa)	Volume Collapse %
CaSe	Experimental [17] Cortona <i>et al.</i> 1998 [37] Charifi <i>et al.</i> 2005 [35]	38 45 34.4-40.6	7.7 7.1 5.8
	Varshney et al. 2009 [160] Khenata et al. 2006 [9] Hao et al. 2010 [180] Potzel et al. 2011 [176]	38 35.2 37.5 39.7	4.5 - - -
	Bhardwaj et al. 2010 [169]	37.7	7.2
СаТе	Experimental [17] Cortona et al. 1998 [37] Charifi et al. 2005 [35] Varshney et al. 2009 [160] Khenata et al. 2006 [9] Hao et al. 2010 [180] Potzel et al. 2011 [176] Bhardwaj et al. 2010 [169]	33 27 30.4-31.6 34 30.2 33.0 38.4 32.9	4.6 6.1 6.2 6.7 - - - 4.3
MgS	Zimmer et al. 1985 [14] Varshney et al. 2008 [160] Bhardwaj et al. 2008 [167]	172 167 143	- 6.9 5.2
MgSe	Experimental [39] Zimmer et al. 1985 [14] Varshney et al. 2008 [160] Bhardwaj et al. 2008 [167]	107±8 175 170 156	- - 3.6 3.6
MgTe	Experimental [17] Varshney et al. 2008 [160] Bhardwaj et al. 2008 [167]	>60 176 68.2	5.6 5.6
SrO	Experimental [55] Kalpana <i>et al.</i> 1994 [155] Kholiya <i>et al.</i> 2011 [172] Potzel <i>et al.</i> 2011 [176] Bhardwaj <i>et al.</i> 2009 [165]	36.0 31.7 35.3 30.9 78	13 11.4 - - - 4.75
CaO	Experimental [61] Kalpana <i>et al.</i> 1994 [155] Luo <i>et al.</i> 1994 [17] Liu Ji-Ziang <i>et al.</i> 2007 [46] Potzel <i>et al.</i> 2011 [176] Bhardwaj <i>et al.</i> 2009 [165]	53-70 55.7 61 66.7 59.5 62.8	10 10.7 10 - - - 5.61
ВаО	Experimental [61] Bhardwaj et al. 2008 [166]	85 84	3.3 2.89
MgO	Experimental [55] Kalpana <i>et al.</i> 1994 [155] Bhardwaj <i>et al.</i> 2009 [165]	>1000 197.5 205	5.4 5.5

second order elastic constants and bulk modulus, and volumes for B1 phase are summarized in Table 2, Table 3 and Table 4 respectively for group II-IV alkaline earth chalcogenides. The values given in Tables 2-4 have been calculated by different electronic and model calculations like ab-initio pseudopotential density functional theory, quasi harmonic Debye model, FP-LAPW with GGA, first principle calculation based on DFT with plane wave basis, periodic crystal 98 program, two body potential model, three-body potential model, modified three-body potential model, effective interionic interaction potential, tight binding linear muffintin orbital (TBLMTO) method, etc. Various results of these

calculations have been compared with experimental data for the present group of compounds. The experimental results of phase transitions are available for the present group of compounds except for MgS.

The first order phase transition involving a discontinuity in volume takes place at the transition pressure. Experimentally, one usually studies the relative volume changes $(-\Delta V/V_0)$ associated with the compressions. The discontinuity in volume $(-\Delta V/V_0)$ at the transition pressure is obtained from the phase diagram. The negative sign shows compression in crystal. This is the characteristic of first order phase transition. Various theoretical calculations have been compared here with

 Table 3. Elastic constants and bulk modulus for B1 phase.

Solid	Reference	C ₁₁	C ₁₂	C ₄₄	
SrS	Straub <i>et al.</i> 1989 [26]	192.9	66.1	61.3	
	Khenata et al. 2003 [22]	141.0	17.2	62.5	
	Marinelli et al. 2003 (HF) [38]	117	17	35	
	Marinelli et al. 2003 (LVWN) [38]	150	16	31	
	Marinelli et al. 2003 (PW) [38]	130	11	31	
	Marinelli <i>et al.</i> 2003(B3LYP) [38] Rached <i>et al.</i> 2004 [45]	118 76.1	15 43.6	34 12.7	
	Cheng et al. 2004 [45]	113.9	19.4	30.3	
	Varshney et al. 2008 [160]	90.9	21.3	27.6	
	Bhardwaj <i>et al.</i> 2009 [167]	130.1	12.8	49.86	
SrSe	Straub et al. 1989 [26]	149.9	51.5	48.8	-
0.00	Marinelli <i>et al.</i> 2000 [23]	97.2	16.0	28.6	
	Khenata et al. 2003 [22]	120.0	13.4	53.7	
	Marinelli et al. 2003 (HF) [38]	97	16	29	
	Marinelli et al. 2003 (LVWN) [38]	127	13	27	
	Marinelli et al. 2003 (PW) [38]	107	12	26	
	Marinelli et al. 2003 (B3LYP) [38]	101	14	26	
	Rached et al. 2004 [45]	65.0	37.5	10.6	
	Varshney et al. 2008 [160]	105.6	21.1	28.2	
	Bhardwaj et al. 2009 [167]	116.0	13.5	33.8	-
SrTe	Straub et al. 1989 [26]	133.4	41.4	39.7	
	Khenata et al. 2003 [22]	101.5	7.8	44.8	
	Rached et al. 2004 [45]	52.1	32.8	6.2	
	Varshney et al. 2008 [160]	67.1	13.7	19.8	
	Bhardwaj et al. 2009 [167]	95.02	6.14	40.19	
BaS	Straub et al. 1989 [26]	179.12	58.16	53.99	
	Khenata et al. 2006 [9]	86.8	16.9	31.60	
	Hassan et al. (GGA) 2006 [151]	101.05	9.67	9.24	
	Hassan et al. (LDA) 2006 [151]	115.27	15.04	14.27	
	Benamrani et al. 2010 [146]	115.78	18.18	18.38	
	Baohemadau <i>et al.</i> 2006 [170]	115	17	18	
	Bhardwaj et al. 2008 [166]	108.89	35.06	32.43	-
BaSe	Straub et al. 1989 [26]	139.07	45.02	42.62	
	Hassan <i>et al.</i> (GGA) 2006 [151]	94.74	8.20	8.29	
	Hassan et al. (LDA) 2006 [151]	99.34	8.51	8.38	
	Benamrani <i>et al.</i> 2010 [146] Baohemadau <i>et al.</i> 2006 [170]	112.67 104	14.15 14	15.25 15	
	Bhardwaj <i>et al.</i> 2008 [166]	89.32	4.99	3.86	
BoTo		105.42	35.89	34.29	-
ВаТе	Straub <i>et al.</i> 1989 [26] Hassan <i>et al.</i> (GGA) 2006 [151]	78.54	4.75	4.42	
	Hassan <i>et al.</i> (LDA) 2006 [151]	87.54	5.76	5.34	
	Benamrani et al. 2010 [146]	87.25	9.20	11.38	
	Baohemadau <i>et al.</i> 2006 [170]	87	09	12	
	Bhardwaj et al. 2008 [166]	77.87	3.11	3.95	
0-0					-
CaS	Marinelli et al. 2003 (HF) [38]	113	22	44	
	Marinelli et al. 2003 (LVWN) [38]	170	17	39	
	Marinelli et al. 2003 (PW) [38]	135 127	20	38 40	
	Marinelli et al. 2003 (B3LYP) [38] Charifi et al. 2005 (GGA) [35]	127 108.23	20 32.01	40 36.08	
	Charifi <i>et al.</i> 2005 (GGA) [35]	108.23 122.87	39.66	41.94	
	Hao et al. 2003 (LDA) [33]	123.3	23.6	33.5	
	Khachai <i>et al.</i> 2009 [181]	131.66	31.45	53.94	
	Bhardwaj <i>et al.</i> 2010 [169]	111.12	37.98	39.69	
0000	, , ,				-
CaSe	Marinelli <i>et al.</i> 2000 [23]	109.6-147.0	21.8-22.6	37.6-40	
	Marinelli <i>et al.</i> 2003 (HF) [38]	109	20	36 32	
	Marinelli et al. 2003 (LVWN) [38]	133	18	32	
	Marinelli et al. 2003 (PW) [38] Marinelli et al. 2003 (B3LYP) [38]	115 112	18 18	31 31	
	Charifi <i>et al.</i> 2003 (GGA) [35]	95.17	25.56	27.11	
	Charifi et al. 2005 (LDA) [35]	106.76	23.12	29.90	
	Khenata et al. 2006 [9]	112.6	22.0	34.43	
	Hao et al. 2010 [180]	104.6	20.6	28.5	
	Khachai <i>et al.</i> 2009 [181]	135.06	28.38	57.96	
ı	Bhardwaj et al. 2010 [169]	97.59	26.88	29.12	

Continued Table 3. Elastic constants and bulk modulus for B1 phase.

Solid	Reference	C ₁₁	C ₁₂	C ₄₄
СаТе	Charifi et al. 2005 (GGA) [35]	89.26	14.77	18.52
Cale	Charifi <i>et al.</i> 2005 (LDA) [35]	97.42	17.33	23.99
	Khenata et al. 2006 [9]	92.9	18.4	36.64
	Hao et al. 2010 [180]	86.1	15.8	19.9
	Khachai <i>et al.</i> 2009 [181]	117.9	17.09	54.8
	Bhardwaj et al. 2010 [169]	89.38	14.82	18.86
MgS	Straub <i>et al.</i> 1989 [26]	228.2	105.4	99.3
IVIGO	Marinelli et al. 2003 (HF) [38]	131	50	70
	Marinelli <i>et al.</i> 2003 (LVWN) [38]	164	46	57
	Marinelli <i>et al.</i> 2003 (PW) [38]	146	43	58
	Marinelli et al. 2003(B3LYP) [38]	138	48	63
	Drief et al. 2004 [107]	183.45	34.92	69.01
	Rached et al. 2004 [45]	104-113	75.0-81.3	13.0-14.5
	Varshney et al. 2008 [160]	172.4	24.9	11.6
MaSo				
MgSe	Straub <i>et al.</i> 1989 [26]	172.0	81.1	79.3
	Marinelli et al. 2000 [23]	118-159.6	42-43	56.4-60
	Marinelli et al. 2003 (HF) [38]	118	42	56
	Marinelli et al. 2003 (LVWN) [38]	139 121	37 37	46 47
	Marinelli et al. 2003 (PW) [38] Marinelli et al. 2003 (B3LYP) [38]	121 111	37 36	47 48
	, , , , ,	209.07		
	Drief <i>et al.</i> 2004 [107] Rached <i>et al.</i> 2004 [45]	209.07 84.0-93.1	31.32 61.0-65.7	74.37 11.0-12.5
	Varshney et al. 2008 [160]	148.1	24.1	11.2
	Bhardwaj et al. 2008 [167]	204.23	48.56	54.20
MgTe	Straub et al. 1989 [26]	124.2	65.9	65.9
	Drief et al. 2004 [107]	82.81	25.73	38.96
	Varshney et al. 2008 [160]	96.3	17.6	10.2
	Bhardwaj et al. 2008 [167]	185.36	29.88	31.86
SrO	Experimental [61]	174	47	56
	Mehl et al. 1986 [56]	171	34	49
	Marinelli et al. 2003 (HF) [38]	186	49	68
	Marinelli et al. 2003 (LVWN) [38]	212	47	60
	Marinelli et al. 2003 (PW) [38]	203	40	60
	Marinelli et al. 2003(B3LYP) [38]	192	47	62
	Baltache et al. 2004 [185]	223	46	87
	Bhardwaj et al. 2009 [165]	162	39	47
CaO	Experimental [61]	222	58	80
	Mehl et al. 1986 [56]	206	50	66
	Philippe et al. 1992 [29]	244.7	49.7	99.0
	Marinelli et al. 2003 (HF) [38]	237	59	96
	Marinelli et al. 2003 (LVWN) [38]	290	63	89
	Marinelli et al. 2003 (PW) [38]	226	57	84
	Marinelli et al. 2003 (B3LYP) [38]	219	61	86
	Liu Ji-Ziang et al. 2007 [46]	207	58	76
	Baltache et al. 2004 [185]	274	54	53
	Bhardwaj et al. 2009 [165]	218	52	77.2
ВаО	Experimental [61]	174	49	34
	Mehl et al. 1986 [56]	133	33	31
	Bhardwaj et al. 2009 [166]	112	45	28
MgO	Experimental [61]	299	96.4	157.1
	Cohen et al. 1976 [44]	226	142	142
	Isaak et al. 1990 [16]	310	119	188
	Karki et al. 1997 [49]	291	90	137
	Karki et al. 1999 [51]	323	92	152
	Karki et al. 2000 [51]	300	93.6	147
	Tsuchiya et al. 2001[11]	318	87	144
	Marinelli et al. 2003 (HF) [38]	326	108	188
	Marinelli et al. 2003 (LVWN) [38]	352	97	168
	Marinelli et al. 2003 (PW) [38]	295	91	158
	Marinelli et al. 2003(B3LYP) [38]	286	102	163
[Baltache et al. 2004 [59]	338	91	118
	Lu et al. 2007 [20]	299.9	94.9	146.0
	Liu et al. 2007 [46]	286.1	93.8	144.9
1			91	118
	Baltache et al. 2004 [185]	338	91	110

Table 4. The transition volumes for B1 and B2 phase, for alkaline earth chalcogenides.

Crystal	V _t (B1)/ V ₀	V_{t} (B2)/ V_{o}
BaS		
Experimental [174]	0.873	0.773
Kalpana et al. 1994 [155]	0.896	0.773
Baohemadau et al. 2006 [170]	0.890	0.753
Hassan et al. 2006 [151]	0.896, 0.877	0.771, 0.744
Benamrani et al. 2010 [146]	0.884, 0.985	0.760, 0.785
Kholiya <i>et al</i> . 2011 [172]	0.878	0.786
BaSe		
Wei et al. 1985 [154]	0.89	_
Kalpana et al. 1994 [155]	0.88	0.760
Baohemadau <i>et al</i> . 2006 [170]	0.88	0.785, 0.762
Hassan <i>et al.</i> 2006 [151]	0.901, 0.886	0.762
Benamrani <i>et al</i> . 2010 [146]	0.878, 0.926	0.763, 0.787
Kholiya et al. 2011 [172]	0.886	0.763
	0.000	0.707
BaTe	0.005	0.000
Wei et al. 1985 [154]	0.925	0.800
Kalpana et al. 1994 [155]	0.894	0.798
Akbarzadeh et al. 2000 [158]	0.850	0.78
Baohemadau et al. 2006 [170]	0.886	0.753
Hassan <i>et al.</i> 2006 [151]	0.912, 0.880	0.756, 0.759
Benamrani et al. 2010 [146]	0.883, 0.919	0.775, 0.797
Kholiya <i>et al</i> . 2011 [172]	0.886	0.787
SrS		
Experimental [174]	0.815	0.722
Banu <i>et al</i> . 1998 [86]	0.78	0.692
SrSe		
Experimental [174]	0.813	0.725
Banu et al. 1998 [86]	0.796	0.710
SrTe		
Experimental [174]	0.82	0.729
Zimmer et al. 1985 [14]	0.828	0.876
Banu <i>et al.</i> 1998 [86]	0.8	0.736
CaS		
Experimental	0.730	0.900
Cortona et al. 1998[37]	0.720	-
Charifi et al. 2005[35]	0.720, 0.710	0.904
	0.720, 0.710	0.904
CaSe	0.70	0.04
Experimental	0.70	0.91
Cortona et al. 1998 [37]	0.690	-
Charifi et al. 2005 [35]	0.740, 0.680	0.911
СаТе		
Experimental	0.74, 0.70	
Zimmer <i>et al</i> . 1985 [14]	0.703	0.865
Cortona et al. 1998 [37]	0.73	-
Charifi <i>et al</i> . 2005 [35]	0.72, 0.68	-
Hao et al. 2009	0.750	0.93
MgS		
Kalpana et al. 1994 [155]	0.880	0.750
MgSe		
Kalpana et al. 1994 [155]	0.860	0.740
Van Camp <i>et al</i> . 1997 [171]	0.528	0.510
MaTe		
Van Camp <i>et al</i> . 1997 [171]	0.622	0.588
Chaudhuri et al. 1999	0.479	0.465
	1	5.150

experimental results of volume change with the variation of pressure. This variation of volume change with pressure for barium, strontium, calcium and magnesium chalcogenides have been plotted in Figs. 4a-4d, 5a-5d, 6a-6d and 7a-7d, respectively. It is clear from these figures that the experimental and different theoretical calculations [170-202] show similar trends.

The second order elastic constants and bulk modulus of the present group of compounds have been

summarized in Table 3. Different theoretical values have been compared with experimental study. The experimental results of second order elastic constants are available only for BaO, CaO, SrO and SrSe compounds. Various results of transition volumes V_t (B1)/ V_0 and V_t (B2)/ V_0 are summarized in Table 4 for barium, strontium, calcium and magnesium chalcogenides. The results are compared with the experimental predictions (V_0 is the experimental equilibrium volume for the B1 phase). The

Table 5. Transition volumes (Å)3 for B1 and B2 phase, volume change and energy change for alkaline earth chalcogenides.

Crystal	V _{T1} (Å) ³	V _{T2} (Å) ³	ΔV	ΔΕ
BaS				
Experimental [14]	58.42	50.40	13.7	-
Kalpana <i>et al</i> . 1994 [155]	54.41	48.18	13.8	-
Khenata et al. 2006 [9]	58.74	50.35	14.29	0.38
SrS				
Experimental [152]	44.57	39.49	11.4	-
Banu et al. 1998 [86]	40.03	35.51	11.28	0.568
Khenata et al. 2003 [22]	44.56	39.64	11.04	0.578
SrSe				
Experimental [17]	49.29	43.96	10.70	-
Banu et al. 1998 [86]	45.85	40.89	10.8	0.504
Khenata et al. 2003 [22]	50.33	45.97	8.66	0.494
SrTe				
Experimental [17]	60.62	53.89	8.0	-
Zimmer et al. 1985 [14]	-	-	11.1	_
Banu et al. 1998 [86]	56.78	52.23	11.1	0.392
Khenata et al. 2003 [22]	62.83	58.24	7.30	0.300
CaSe				
Experimental	36.26	_	7.7	_
Kalpana <i>et al</i> . 1994 [155]	34.42	32.32	6.1	0.7
Khenata <i>et al.</i> 2006 [9]	38.36	36.15	5.8	0.65
CaTe				
Experimental	47.37	_	4.6	
Zimmer <i>et al.</i> 1985 [14]	-	_	10.8	_
Kalpana <i>et al.</i> 1994 [155]	41.23	39.16	4.43	-
Khenata et al. 2006 [9]	45.33	42.51	6.2	0.675
MgSe	1			
Van Camp <i>et al</i> . 1997 [171]	3.50	_		0.374
MqTe	0.00			0.074
мете Van Camp <i>et al</i> . 1997 [171]	5.52	-	-	0.380
CaO				
Experimental [193]	27.83	24.57	_	_
Mehl et al. 1986 [56]	27.99	24.97	_	_
Mehl et al. 1988 [192]	26.53	23.16	_	_
Philippe et al. 1992 (MURN) [29]	29.66	26.20	_	_
Philippe et al. 1992 (BM2) [29]	30.32	26.54	-	-
Philippe et al. 1992 (BM3) [29]	29.88	26.26	-	-
Philippe et al. 1992 (D & G) [29]	30.02	26.28	-	-
Philippe et al. 1992 (B) [29]	29.86	26.25	-	-
Philippe et al. 1992 (S) [29]	29.99	26.28	-	-
1-1				

results on transition volumes are available theoretically for barium, strontium, calcium and magnesium chalcogenides except for divalent metal oxides. The results on transition volumes are available experimentally only for BaSe, BaTe, SrS, SrSe, SrTe, CaS, CaSe, and CaTe compounds. The values of transition volumes V_{t1} and V_{t2} (in ų), volume change (Δ V), and energy change (Δ E) for alkaline earth chalcogenides have also been given in Table 5 and compared our results with others data [14,35,37,86,146,151,155,170-172].

The variation of phase transition pressure and volume change for available values has been plotted for barium, strontium, calcium and magnesium chalcogenides and divalent metal oxides in Figs. 8 and 9. It is clear from the figures that experimental and theoretical studies show almost the same movement in their behavior. In Fig. 10, the variation of bulk modulus for barium, strontium, calcium and magnesium chalcogenides and

divalent metal oxides have been plotted and compared with experimental results. Both studies represent similar behavior.

7. Conclusion

In the present work, an effort has been made to review the experimental and theoretical investigations of the pressure induced phase transition and the mechanical properties of the ionic crystals. A survey of literature reveals that a large amount of experimental work has been done on the phase transition and mechanical properties of alkaline earth chalcogenides. Besides the various types of electronic and model calculations, these have also been performed using different types of approaches. Each and every study has some limitations in their work and further efforts have been

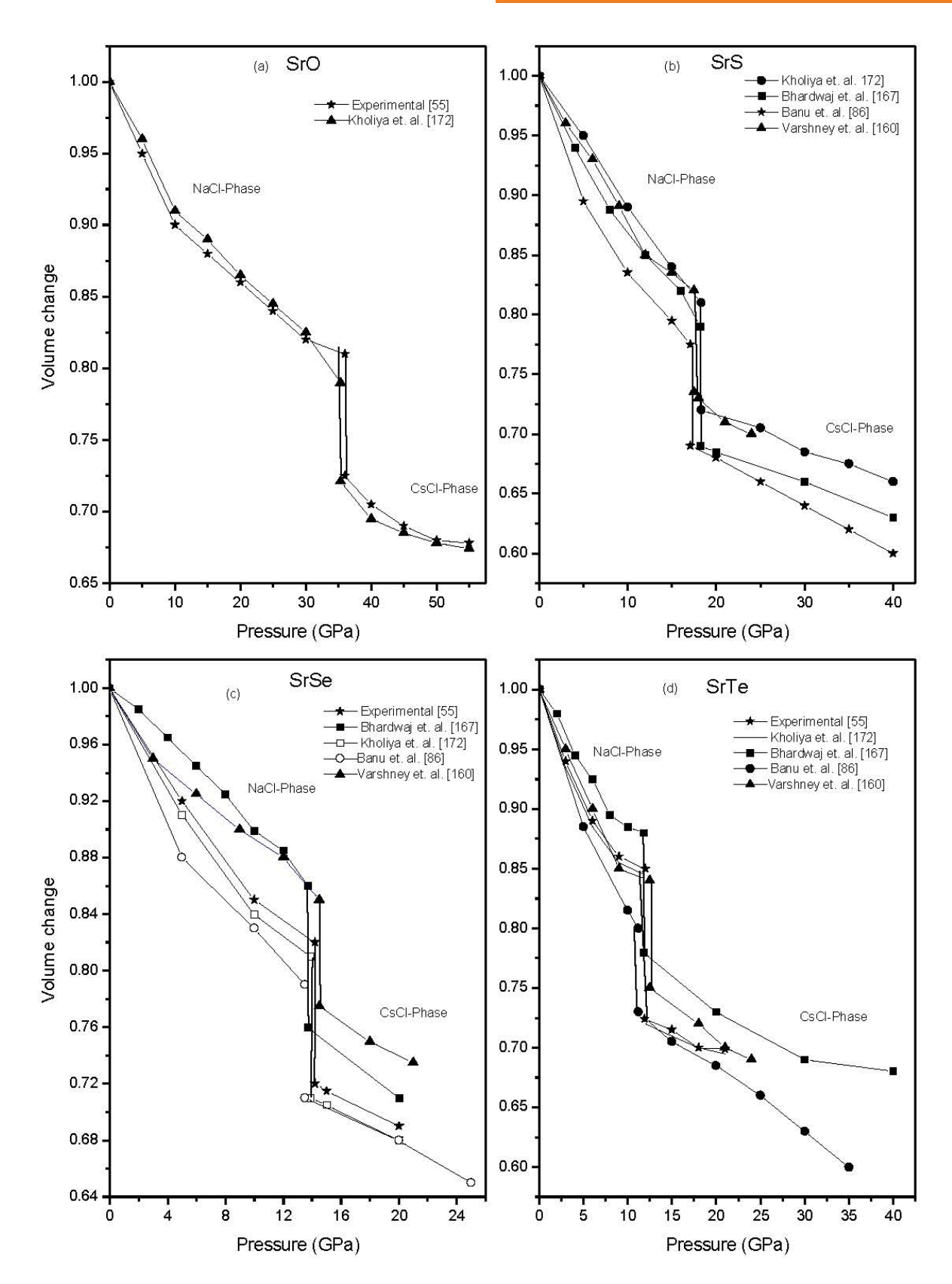


Figure 4. Variation of volume collapse with pressure for barium chalcogenides.

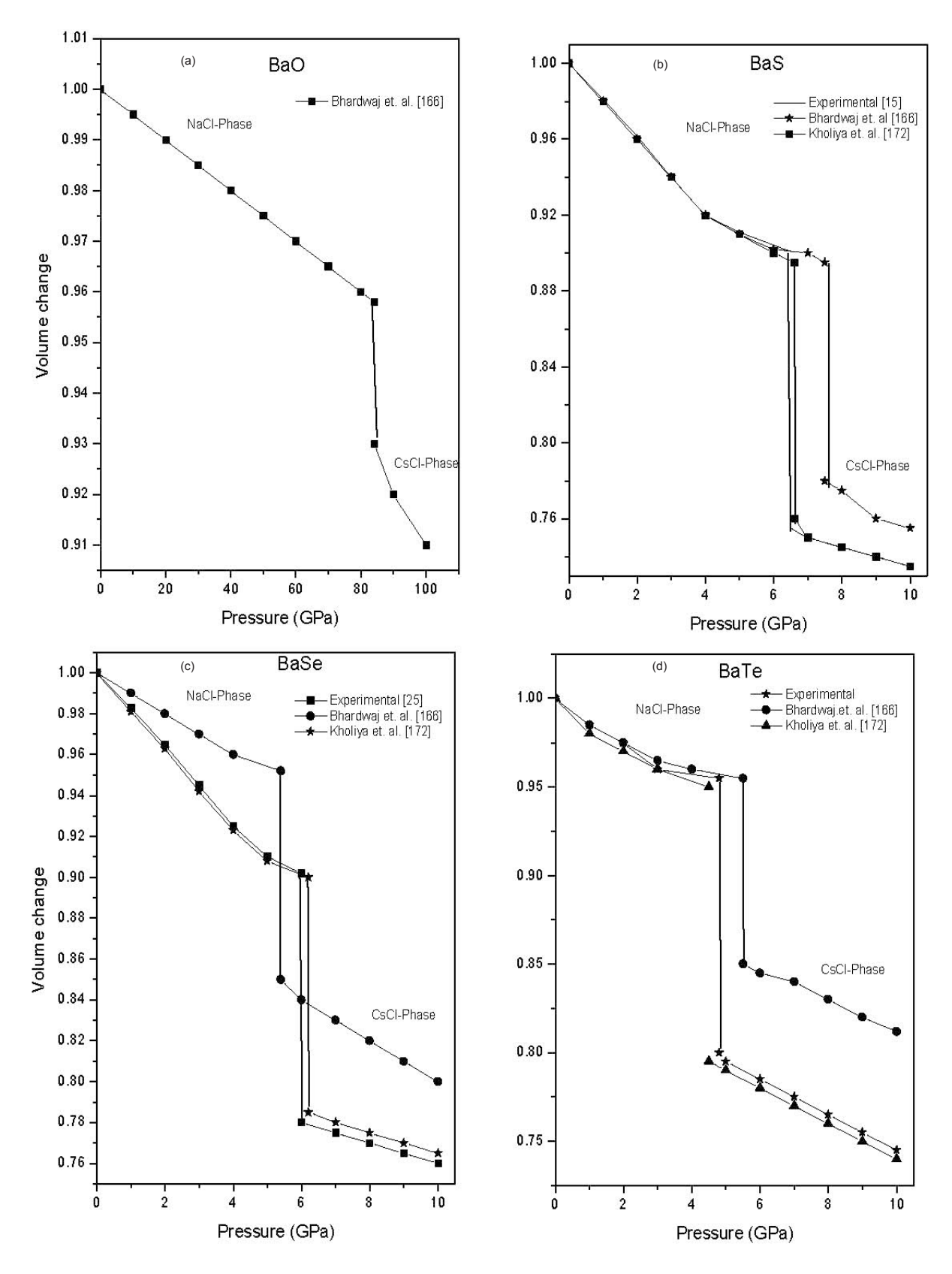


Figure 5. Variation of volume collapse with pressure for strontium chalcogenides.

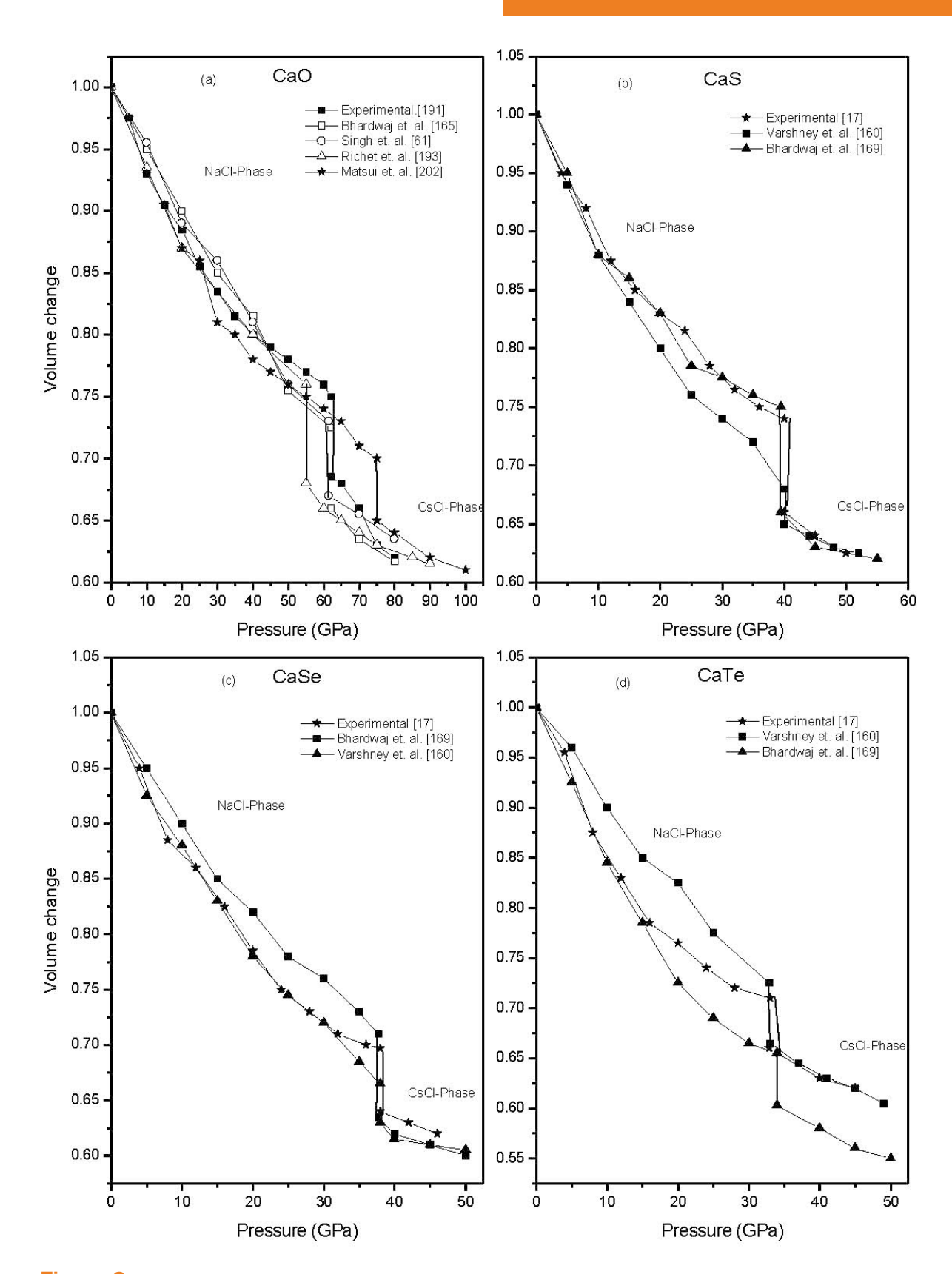


Figure 6. Variation of volume collapse with pressure for calcium chalcogenides.

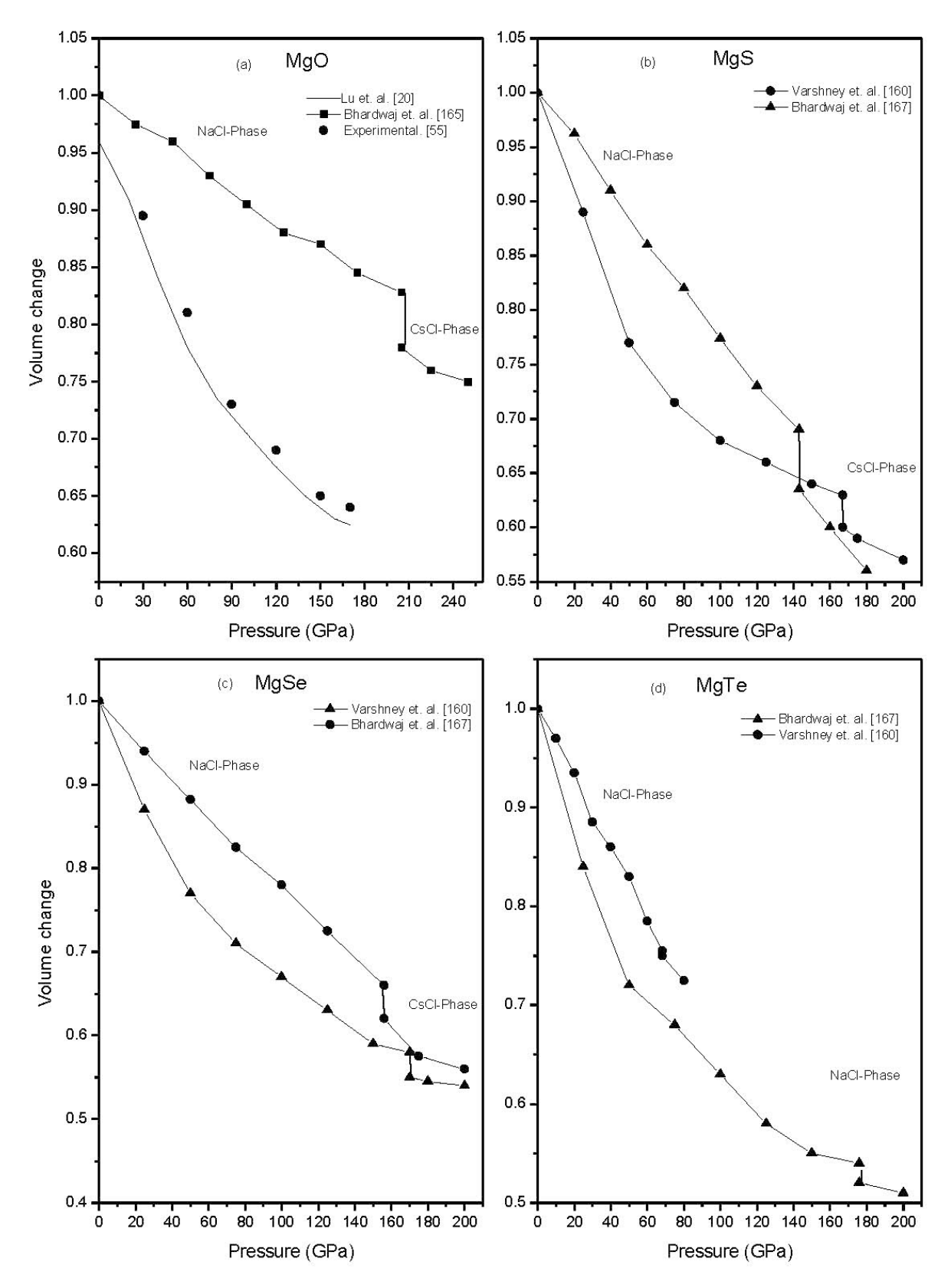


Figure 7. Variation of volume collapse with pressure for magnesium chalcogenides.

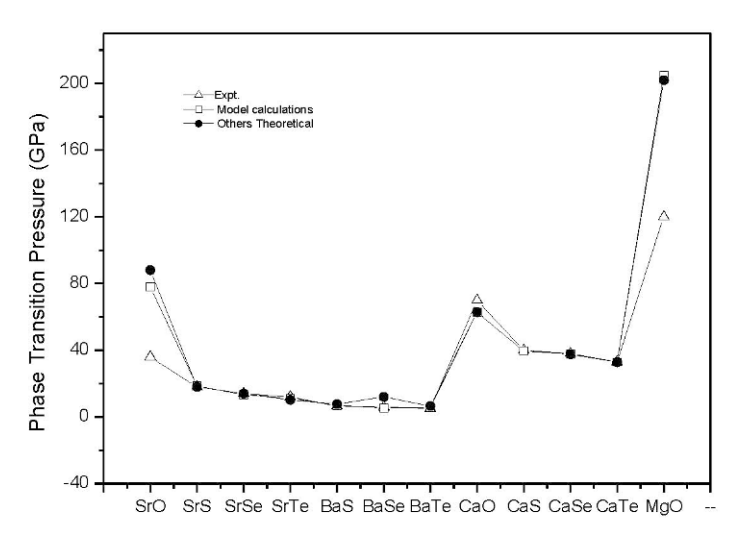


Figure 8. Phase transition pressure of alkaline earth chalcogenides.

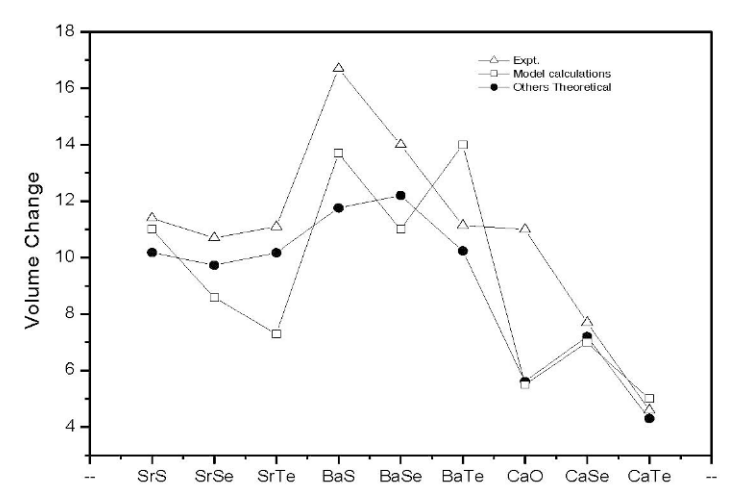


Figure 9. Volume collapse of alkaline earth chalcogenides.

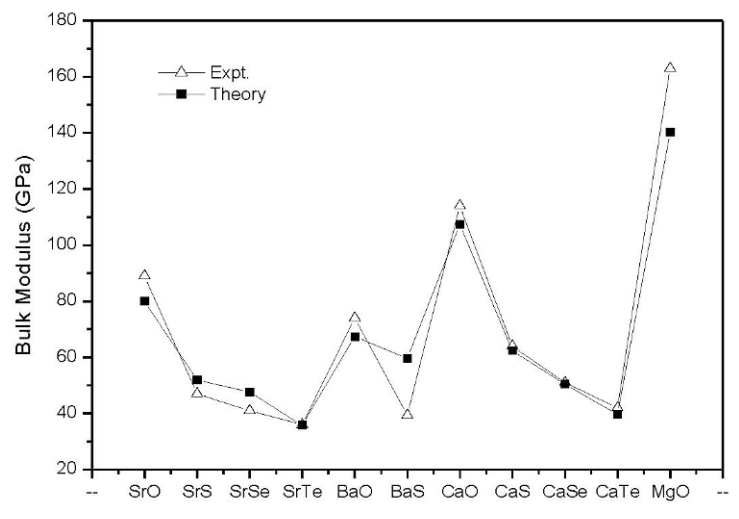


Figure 10. Phase transition pressure and Volume collapse of alkaline earth chalcogenides.

made to overcome these limitations. Few workers have investigated the structural phase transition in alkaline earth chalcogenides using the pseudo potential total energies method within the local density approximation. The first principle calculations have successfully predicted the electronic band structure, energy band gap and elastic properties of alkaline earth chalcogenides. While the first-principles calculations can envisage the electronic properties of ionic compounds acceptably, the significance of van der Waals (vdW) attraction due to the dipole-dipole (d-d) and dipole-quadruple (d-q) interactions to describe the cohesion in ionic solids are generally ignored in the first principle calculations. This attraction has been successfully included in the model calculations.

The developments in theoretical modelling have made promising the calculation of structural, mechanical and thermal properties of different groups of compounds. For the calculation of elastic moduli, models based on two body central forces necessarily fail to reproduce the measured deviation from the Cauchy inequality C₁₃≠C₄₄ for cubic crystals. These workers have achieved successful predictions of phase transition pressures and concluded that minor deviation might be due to the exclusion of the effect of non-rigidity of ions in the model. The effect of such a non-rigidity of ions via three body interaction have been incorporated in the successful study of the phase transition and mechanical properties of alkaline earth chalcogenides. In modified interaction potential model, both types of interactions, long range as well as short range (the overlap repulsive interaction effective up to next neighbors), have been taken under consideration. The Cauchy discrepancy has been successfully overcome by the three body potential approach. The three body potential model has successfully predicted the phase transition, volume collapse, elastic and thermal properties of alkaline earth chalcogenides for rock salt (NaCl), cesium chloride (CsCl) and Zinc blend (ZnS) phases, but it is insufficient to predict these properties for other structures i.e. tetragonal, orthorhombic, hexagonal, etc. The comparative study of percentage of relative

volume changes using the compression curves have been presented in Table 2. The overall achievements presented in this work give rise to clear evidence of the appropriate review of high pressure structural phase transition and the elastic properties of ionic crystals.

In summary, we have summarized the results as follows:

- 1. On the entire contract between theory and experiment is in general terrific. There are inconsistencies, some of which definitely result from insufficiency in the calculations, but overall it is not an overstatement to say that density-functional theory and first-principles calculations are successful to study the high pressure structural behaviour of ionic compounds.
- As the FLAPW-GGA method, it may not provide the correct description of strongly correlated systems and may overestimate the magnetic contributions to the total energy for some 3d metals and their compounds.
- 3. First-principles calculations of high-pressure phases have been useful in testing and aiding the development of other theoretical methods. For example, first-principles data on the energies of different phases have been used in the fitting of parameters for tight-binding models and empirical potentials.
- 4. Whereas the first-principles calculations can predict the electronic properties of ionic compounds acceptably, the significance of Van der Waals attraction to describe the cohesion in ionic solids are generally ignored in the first principle calculations.
- 5. This Van der Waals attraction has been successfully included in the model calculations.
- 6. The model calculations are also required to describe covalent, ionic, and metallic bonded materials. The interatomic forces are well explained through model calculations.

Acknowledgement

One of the authors (PB) is grateful to the Department of Science & Technology (DST), New Delhi for awarding WOS- 'A' and the financial support to this work.

References

- [1] A.J. Dekkar, Solid State Physics (Macmillan, Madras, 1970)
- [2] C. Kittel, Introduction to Solid State Physics, 5th edition (Wiley Eastern, New Delhi, 1998)
- [3] M.A. Omar, Elementary Solid State Physics: Principles and Applications, 7th edition (Addison-Wesley, U.S.A., 2005)
- [4] W.B. Holzapfel, Rep. Prog. Phys. 59, 29 (1996)
- [5] A. Mujica Angel Rubio, A. Munoz, R.J. Needs, Reviews of Modern Physics 75, 863 (2003)
- [6] N.V. Chandra Shekhar, K. Govind Rajan, Bull. Mater. Sci. 24, 1 (2001)
- [7] M.T. Yin, M.L. Cohen, Phys. Rev Lett. 45, 1004 (1980)
- [8] M. Dadsetani, A. Pourghazi, Phys. Rev. B 73, 195102 (2006)

- [9] R. Khenata, H. Baltache, M. Rerat, M. Driz, B. Sahnoun, B. Bouhafs, B. Abbar, Physica B 371, 12 (2006)
- [10] A. Chakrabarti, Phys. Rev. B 62, 1806 (2000)
- [11] T. Tsuchiya, K. Kawamura, J. Chem. Phys. 114, 10086 (2001)
- [12] G.A. Saum, E.B. Hensley, Phys. Rev. 113, 1019 (1959)
- [13] B.S. Rao, S.P. Sanyal, Phys. Stat. Sol. 165, 369 (1991)
- [14] H.G. Zimmer, H. Winze, K. Syassen, Phys. Rev. B 32, 4066 (1985)
- [15] S. Yamaoka, O. Shimomura, H. Nakazawa, O. Fukunaga, Solid State Commun. 33, 87 (1980)
- [16] O.L. Anderson, D.G. Isaak, H. Oda, J. Geophys. Res. 96, 18037 (1991)
- [17] H. Luo, R.G. Greene, K. Ghandehari, T. Li, A.L. Ruoff, Phys. Rev. B 50, 16232 (1994)
- [18] Y. Cheng, L.-Y. Lu, O.-H. Jia, Q.-Q. Gou, Commun. Theor. Phys. 49, 1611 (2008)
- [19] X.-C. Yang, A.-M. Hao, J.H. Yang, Y.-H. Peng Gang, C.-X. Gao, G.-T. Zou, Chin. Phys. Lett. 25, 1807 (2008)
- [20] L.-Y. Lu, J.-J. Tan, O.-H. Jia, X.-R. Chen, Physica B 399, 66 (2007)
- [21] Y.-D. Guo, Z.-J. Yang, Q.-H. Gao, Z.J. Liu, W. Dai, J Phys.: Condens. Matter 20, 115203 (2008)
- [22] R. Khenata, H. Baltache, M. Rerat, M. Driz. M. Sahnoun, B. Bouhafs, B. Abbar, Physica B 339, 208 (2003)
- [23] F. Marinelli, H. Dupin, A. Lichanot, J. Phys. Chem. of Solids 61, 1707 (2000)
- [24] T.A. Grzybowski, A.L. Ruoff, Phys. Rev. B 27, 6502 (1983)
- [25] T.A. Grzybowski, A.L. Ruoff, Phys. Rev. Lett. 53, 489 (1984)
- [26] G.K. Straub. W.A. Harrision, Phys. Rev. B 39, 10325 (1989)
- [27] Y. Deng, O.-H. Jia, X.-R. Chen, J. Zhu, Physica B 392, 229 (2007)
- [28] L. Pauling, The nature of the chemical bond, (Cornell University Press, Ithaca, 1960)
- [29] P. D'Arco, L.-H. Jolly, B. Silv, Physics of the Earth and Planetary interiors 72, 286 (1992)
- [30] W.E. Moffitt, Proc. Roy. Soc. London 202, 548 (1950)
- [31] A.W. Streitwieser, Jr. Molecular orbital theory (Wiley, New York, 1961)
- [32] (a) P.O. Lowdin, Adv. Phys. 75, 1 (1932); (b) P.O. Lowdin, J. Chem. Phys. 18, 113 (1961)
- [33] S.O. Lundqvist, Ark. Fys. (Swedon) 12, 365 (1958)
- [34] A.B.D. Woods, W. Cochren, B.N. Brochhous, Phys. Rev. B 119, 980 (1960)

- [35] Z. Charifi, H. Baaziz, F. El Haj Hassan, N. Bouarissa, J. Phys.: Condens. Matter 17, 4083 (2005)
- [36] S. Singh, R.K. Singh, J. Phys. Soc. Jpn. 71, 2477 (2002)
- [37] P. Cortona, P. Masi, J. Phys.: Condens. Matter 10, 8947(1998)
- [38] F. Marinelli, A. Lichanot, Chem. Phys. Lett. 367, 430 (2003)
- [39] T.S. Tuffy, R.J. Hamely, H. Mao, Phys. Rev. Lett. 74, 1371 (1995)
- [40] A. Khun, A. Chevy, M.J. Naud, J. Cryst. Growth 9, 623 (1971)
- [41] T. Li, Luo, R.G. Green, A.L. Ruoff, S.S. Trail, F.J. DiSalvo, Phys. Rev. Lett. 74, 5232 (1995)
- [42] C.Y. Yeh, Z.W. Lu, S. Froyen, A. Zunger, Phys. Rev. B. 46, 10086 (1992)
- [43] R. Pandey, A. Sutjianto, Solid State Commun. 9, 269 (1994)
- [44] A.J. Cohen, R.G. Gordon, Phys. Rev. B 12, 3228 (1975)
- [45] D. Rached, M. Rabah, N. Benkhettou, B. Soudini, H. Abid, Physica Status Solidi 241, 2529 (2004)
- [46] Z.-J. Liu, J.-H. Qi, Y. Guo, Q.-F. Chen, L.-Ch. Cai, X.-D. Yang, Chinese Physics 16, 499 (2007)
- [47] K.J. Chang, M.L. Cohen, Phys. Rev. B 30, 4774 (1984)
- [48] B.B. Karki, R.M. Wentzcovitch, Phys. Rev. B 68, 224304 (2003)
- [49] B.B. Karki, G.J. Ackland, J. Crain, J. Phys.: Condens. Matter 9, 8579 (1997)
- [50] J. Shankar, S.S. Kushwah, P. Kumar, Physica B 233, 78 (1997)
- [51] (a) B.B. Karki J. Geo. Res. 104, 13025 (1999);(b) B.B. Karki, R.M. Wentzcovitch, Phys. Rev. B 61, 8793 (2000)
- [52] M. Alfredsson, J.P. Brodholt, P.B. Wilson, G.D. Price, F. Cora, M. Calleja, R. Bruin, L. J. Blanshard, R.P. Tyers. Molicular simulation 31, 367 (2005)
- [53] F.D. Stacey, Physics of the earth (Wiley, New York, 1969)
- [54] K.H. Rider, B.A. Weinstein, M. Cardona, H. Bilz, Phys. Rev. B. 8, 4780 (1973)
- [55] Y. Sato, R. Jeanloz, J. Geophys. Res. 86, 11773 (1981)
- [56] M.J. Mehl, L.L. Boyer, H.K. Krakauer, Bull. Am. Phys. Soc. 31, 496 (1986)
- [57] X. Bukowinski, Geophys. Res. Lett. 12, 536 (1985)
- [58] R.J. Hamely, M.D. Jackson, R.G. Gordon, Geophys. Res. Lett. 12, 241 (1985)
- [59] W.J. Carter, S.P. Marsh, J.N. Frity, R.G. McQueen, Natl. Bur. Stand. (U.S.) Circ. No.326, 147, (1971)
- [60] H.K. Mao, P.M. Bell, J. Geophys. Res. 84, 4533

- (1979)
- [61] K.N. Jog, R.K. Singh, S.P. Sanyal, Phys. Rev. B 31 (1985) 6047
- [62] R. Jeanloz, T.J. Ahrens, H.K. Mao, P.M. Bell, Science 206, 829 (1979)
- [63] C.N.R. Rao, K.J. Rao, Phase transition in solids (McGraw Hill, New York, 1978)
- [64] C.M. Waymen, Introduction to the crystallography of Martensitic Transformations (McMillan, New York, 1964)
- [65] G. Mayrick, G.W. Powell, In: R.A. Hugins, R.W. Bube, R.W. Roberts (Eds.), Ann. Rev. Material Science 3, 377 (1975)
- [66] J.E. Ricci, The phase rule and heterogeneous equilibria (Van Nostrand, New York, 1951)
- [67] P. Ehrenfest, Proc. Amsterdam Acad. 36, 153 (1933)
- [68] M.J. Buerger, Fortschr. Miner 39, 9 (1961)
- [69] M.J. Buerger, Phase Transitions in Solids (Wiley, New York, 1951)
- [70] M. Bornard, K. Huang, Dynamical Theory of Crystal Lattices (Oxford University Press, Clarendon, 1954)
- [71] M.P. Tosi, Solid State Physics 16, 1 (1984)
- [72] J.C. Philips, Rev. Mod. Phys. 42, 317 (1970)
- [73] J.C. Philips, Bond and Bands in semiconductors (Academic Press, New York, 1973)
- [74] P.W. Bridgman, The effect of high pressure (Macmillan, New York, 1952)
- [75] H. Brook, F. Birch, G. Holton, W. Paul, Collected experimental papers of P.W. Bridgman (Harvard University Press, Cambridge, 1964) 7
- [76] R.H. Wentorf, Modern very high pressure techniques (Butterworth's, Washington, 1963)
- [77] H.L. Skriver Phys. Rev. B 31, 1909 (1985)
- [78] S.C. Gupta, In: S.C. Schmidt, R.D. Dick, J.W. Forbes, D.G. Tasker (Eds.), Shock compression of condensed matter (Elsevier, Amsterdam, 1992) 157
- [79] S.C. Gupta, J.M. Daswani, S.K. Sikka,R. Chidambaram, Curr. Sci. 65, 399 (1993)
- [80] J.S. Tse, D.D. Khy, Phys. Rev. Lett. 67, 3551 (1991)
- [81] S.L. Chaplot, S.K. Sikka, Phys. Rev. B 47, 5710 (1993)
- [82] S.L. Chaplot, S.K. Sikka, In: A.K. Singh (Ed.), Recent trends in high pressure research, Proc. of the XIII AIRAPT conference on high pressure science and technology (IBH, New Delhi, Oxford, 1992) 259
- [83] A.W. Czenderna, C.N.R. Rao, J.M. Horing, Trans. Faraday Soc. 54, 1069 (1958)
- [84] H.K. Heinish, R. Roy, L.E. Cross (Eds.), Phase

- transitions (VCH, New York, 1973) 5
- [85] C.R. Rao, K.J. Rao (Ed.), Prog. In Solid State. Chem. (Pergamon Press, London, 1967) 4
- [86] I.B. Shameem Banu, M. Rajagopalan, B. Palanivel, G. Kalpana, P. Shenbagaraman Journal of Low Temperature Physics 112, 211 (1998)
- [87] S.C. Gupta, R. Chidambaram High Press. Res. 12, 51 (1994)
- [88] R. Pynn, Nature 281, 5731 (1979)
- [89] W.L. McMillan Phys. Rev. B 14, 1416 (1976)
- [90] Z. Petzelt, Phase Transitions 2, 155 (1981)
- [91] R.A. Cowley, A.D. Bruce, J. Phys. C: Solid State Phys. 11, 3577 (1978)
- [92] Collected papers of P.W. Bridgman (Harvard Univ. Press, Cambridge, 1964)
- [93] P.W. Bridgman, High Pressure Engineering (The institution of Mechanical engineers, London, 1968) part 3C, 182
- [94] Y.K. Yogurtcu, A.J. Miller, G.A. Saundres, J. Phys. Chem. Solids 42, 49 (1981)
- [95] Z.P. Chang, E.K. Graham, J. Phys. Chem. Solids 38, 1355 (1977)
- [96] M.H. Rice, R.G. Mc. Queen, J.M. Walsh, Solid State Physics 47, (1975)
- [97] S.N. Vaidya, V. Vijay Kumar, C. Karunakaran, BARC, Reports 102, 1 (1981)
- [98] J. Xu, H.K. Mao, P.M. Bell, Science 232, 1401 (1986)
- [99] A.L. Ruoff, H. Xia, Q. Xia, Rev. Sci. Instrum. 63, 4342 (1992)
- [100] I.L. Spain, Contemp. Phys. 232, 1401 (1986)
- [101] S. Scandolo, M. Bernasconi, G.L. Chiarotti, P. Focher, E. Tossatti, Phys. Rev. Lett. 74, 4015 (1995)
- [102] G.F. Molinar, L. Bianchi, Physica 140, 743 (1986)
- [103] S. Singh, R.K. Singh, B.P. Singh, S.K. Singhal, R. Chopra, Phys. Stat. Sol. 180, 459 (2000)
- [104] D.S. Rimai, D.J. Sladek, Solid State Commun. 30, 591 (1979)
- [105] P.C. Sahu et al., Rev. Sci. Instrum. 64, 3030 (1995)
- [106] N.V. Chandra Shekhar et al., Pramana 40, 367 (1993)
- [107] F. Drief, A. Tadjer, D. Mesri, H. Aourag, Catalysis Today 89, 343 (2004)
- [108] A. Jayaraman, Rev. Sci. Instumn. 57, 1013 (1986)
- [109] G.J. Piermarini, S. Block, J.D. Barnett, J Appl. Phys. 46, 2774 (1975)
- [110] P.C. Sahu, Ph. D, Thesis (University of Madras, Madras, 1994)
- [111] L. Merril, W.A. Basset, Rev. Sci. Instumn 45, 290 (1974)

- [112] (a) R.M. Haszen, C.W. Burham, Science 194, 105 (1974); (b) R.M. Haszenand, L.W. Finger. Rev. Sci. Instumn. 52, 75 (1981)
- [113] B.C. Giessen, G.E. Gordon, Science 159, 973 (1968)
- [114] N.F. Mott, J. Jones, Theory of the properties of metal and alloys (Oxford University Press, Oxford, 1936)
- [115] J.C. Philips, L. Kleinman, Phys. Rev. 116, 287 (1959)
- [116] V. Heine, D. Weaire, Solid State Phys. 24, 249 (1970)
- [117] T. Soma, J. Phys. C 11, 2681 (1978)
- [118] J. Hafner, V. Heine, J. Phys. F: Met. Phys. 13, 2479 (1983)
- [119] M.C. Payne, M.P. Teter, D.C. Allan, T.A. Arias, J.D. Joannopoulos, Rev. Mod. Phys. 64, 1045 (1992)
- [120] W.E. Pickett, Comput. Phys. Rep. 9, 115 (1989)
- [121] P. Hohenberg, W. Kohn, Phys. Rev. 136, 864B (1964)
- [122] R.M. Dreizler, E.K.U. Gross, Density functional theory (Springer, Berlin, 1990)
- [123] W. Kohn, L.J. Sham, Phys. Rev. 140, A1133 (1965)
- [124] R. Car, M. Parrinello, Phys. Rev. Lett. 55, 2471 (1985)
- [125] O. Sugino, R. Car, Phys. Rev. Lett. 74, 1823 (1995)
- [126] P. Focher, G.L. Chiarotti, M. Bernasconi, E. Tosatti, M. Parrinello, Europhys. Lett. 26, 345 (1994)
- [127] S Scandolo, M. Bernasconi, G. L. Chiarotti, P. Focher, E. Tosatti, Phys. Rev. Lett. 74, 4015 (1995)
- [128] W.A. Harrison, W.H. Freeman, Electronic Structure and the Properties of Solids (Dover, New York, 1989)
- [129] W.A. Harrison, In: J. Treusch (Ed.), Solid state theory (Vieweg, Braunschweig, 1977) Vol. XVII, 135
- [130] S. Froyen, W.A. Harrison, Phys. Rev. 820, 2420 (1979)
- [131] W.A. Harrison, Phys. Rev. B 31, 2121 (1985)
- [132] D. Marx, J. Hutter, Modern Methods and Algorithm of Quantum Chemistry 1, 301 (2000)
- [133] W. Kohn, L.J. Sham, Phys. Rev. 140, A1133 (1965)
- [134] L.D. Landu, Sov. Phys. JETP 35, 70 (1959)
- [135] (a) M.S. Hybertsen, S.G. Louie, Phys. Rev. Lett. 55, 1418 (1985); (b) M.S. Hybertsen, S.G. Louie, Phys. Rev. B 37, 2733 (1988)
- [136] R.W. Godby, M. Schluter, L.J. Sham, Phys. Rev. Lett. 56, 2415 (1986)

- [137] M. Van Schilfgaarrde, T. Kotani, S. Fallev, Phys. Rev. Lett. 56, 601 (2006)
- [138] W.R.L. Lambrecht, Phys. Rev. B. 62, 13538 (2000)
- [139] G. Kotliar, S.Y. Savrasov, K. Haule, V.S. Oudovenko, O. Parcollet, C.A. Marianetti, Rev. Mod. Phys. 78, 865 (2006)
- [140] W. Metzner, D. Vollhardt, Phys. Rev. Lett. 62, 324 (1989)
- [141] A. Georges, G. Kotliar, W. Krauth, M.J. Rozenberg, Rev. Mod. Phys. 68, 13 (1996)
- [142] V.I. Anisimov, A.I. Poteryaev, M.A. Jorotin, A.O. Anokhin, G. Kotliar, J. Phys. Condens. Matter 9, 7359 (1997)
- [143] R. Chitra, G. Kotliar, Phys. Rev. B. 62, 12715 (2000)
- [144] V.I. Anisimov, I.V. Solovyen, M.A. Korotin, M.T. Czyzyk, G.A. Sawatzky, Phys. Rev. B. 48, 16929 (1993)
- [145] C.E. Sims, G.D. Barrera, N.L. Allan, Phys. Rev. B 57, 11164 (1998)
- [146] A. Benamrani, K. Kassali, Kh. Bouamama, High Pressure Research 30, 207 (2010)
- [147] (a) R.K. Singh, S. Singh, Phys. Rev. B 39, 671 (1989); (b) R.K. Singh, S. Singh, Phase Transit. 15, 127 (1989)
- [148] K. Motida, J. Phys. Soc. Jpn 55, 1636 (1986)
- [149] K. Motida, J. Phys. Soc. Jpn 56, 1785 (1987)
- [150] P.K. Jha, U.K. Sakalle, S.P. Sanyal, J. Phys. Chem. Solids 59, 1633 (1998)
- [151] F. El Haj Hassan, H. Akbarzadeh, Computational Material Science 38, 362 (2006)
- [152] (a) K. Syassen, N.E. Christensen, H. Winzen, K. Fisher, J. Evers, Phys. Rev. B 35, 4052 (1987);(b) K. Syassen, Phys. Stat. Sol. A 91, 11 (1985);(c) K. Syassen, Phys. Rev. B 35, 4052 (1987)
- [153] S.T. Weir, Y.K. Vohra, A.L. Ruo, Phys. Rev. B 35, 874 (1987)
- [154] S.H. Wei, H. Krakauer, Phys. Rev. Lett. 55, 1200 (1985)
- [155] G. Kalpana, B. Palanivel, M. Rajagopalan, Phys. Rev. B 50, 12318 (1994)
- [156] A.E. Carlsson, J.W. Wilkins, Phys. Rev. B 29, 5836 (1984)
- [157] G.K. Straub, W.A. Harrison, Phys. Rev. B 39, 10325 (1989)
- [158] H. Akbarzadeh, M. Dadsetani, M. Mehrani, Comput. Mater. Sci. 17, 81 (2000)
- [159] W.A. Harrison, Phys. Rev. B 34, 2787 (1986)
- [160] (a) D. Varshney, N. Kaurav, U. Sharmaa, R.K. Singh, Journal of Physics and Chemistry of Solids 69, 60 (2008); (b) D. Varshney, N. Kaurav, U. Sharmaa, R.K. Singh, Computational

- Material Science 41, 529 (2008); (c) D. Varshney, N. Kaurav, U. Sharmaa, R.K. Singh, J. Alloy and Comp. 484, 239 (2009)
- [161] R.D. Shannon, Acta Crystallogr. 32, 751 (1976)
- [162] P. Bhardwaj, S. Singh, Physica B 406, 1615 (2011)
- [163] P. Bhardwaj, S. Singh, J. Alloy Comp. 509, 7047 (2011)
- [164] P. Bhardwaj, S. Singh, Mat. Chem. Phys. 125, 440 (2011)
- [165] P. Bhardwaj, S. Singh, N.K. Gaur, Mat. Res. Bull. 44, 1366 (2009)
- [166] P. Bhardwaj, S. Singh, N.K. Gaur, Cent. Euro. J. Phys. 6, 223 (2008)
- [167] (a) P. Bhardwaj, S. Singh, N.K. Gaur, Journal of Molecular Structure: THEOCHEM 897, 95 (2009); (b) P. Bhardwaj, S. Singh, N.K. Gaur, Turk. J. Phys. 32, 1 (2008)
- [168] P. Bhardwaj, S. Singh, Phys. Status Solidi B 248, 38 (2012)
- [169] P. Bhardwaj, S. Singh, R.K. Singh, J. Opto. Advanced Mat. 12, 1297 (2010)
- [170] A. Bouhemadou, R. Khenata, F. Zegrar, M. Sahnoun, H. Baltache, A.H. Reshak, Computational Materials Science 38, 263 (2006)
- [171] (a) P.E. Van Camp, V.E. Van Doren, Phys. Rev. B 55, 775 (1997); (b) P.E. Van Camp, V.E. Van Doren, Int. J. Quant. Chem. 55, 339 (1995); (c) P.E. Van Camp, V.E. Van Doren, J.L. Martins, Phys. Stat. Sol. B 190, 193 (1995)
- [172] (a) K. Kholiya, S. Verma, Phase Transitions 84, 67 (2011); (b) K. Kholiya, B.R.K. Gupta, Phase Transitions 81, 403 (2008)
- [173] F. Birch, J. Geophys. Res. 83, 1257 (1978)
- [174] S. Yamaoka, O. Shimomuro, H. Nakasawa, O. Fukunaga, Solid State Commun. 33, 87 (1980)
- [175] E. Tuncel, K. Colakoglu, E. Deglioz, Y.O. Ciftci, J. Phys. Chem. Solids 70, 371 (2009)
- [176] O. Potzel, G. Taubmann, Journal of Solid State Chemistry 184, 1079 (2011).
- [177] A.E. Carlsson, J.W. Wilkins, Phys. Rev. B 29, 5836 (1984)
- [178] J. Wang, S. Yip, Phys. Rev. Lett. 71, 4182 (1993)
- [179] S. Baroni, P. Giannozzi, A. Testa, Phys. Rev. 58, 1861 (1987)
- [180] A.M. Hao, X.C. Yang, Z.M. Gao, X. Liu, Y. Zhua, R.P. Liua, High Pressure Research 30, 310 (2010)

- [181] H. Khachai et al., Physics Procedia 2, 921 (2009)
- [182] J.M. Wills, B. Cooper, Phys. Rev. B, 36, 389 (1987)
- [183] R. Panday, P. Lepak, J.E. Jaffe, Phys. Rev. B 46, 4976 (1992)
- [184] L.G. Liu, W.A. Bassett, J. Geophys. Res. 77, 4934 (1972)
- [185] H. Baltache, R. Khenata, M. Sahnoun, M. Driz, B. Abbar, B. Bouhafs, Physica B 344, 334 (2004)
- [186] S. Israel, R. Saravanan, N. Srinivasan, S.K. Mohanlal, J. Phys. Chem. Solids 64, 879 (2003)
- [187] P.R. Son, R.A. Partels, J. Phys. Chem. Solids 33, 819 (1972)
- [188] M. Uludog, T. Cag, A. Strachan, A. William Goddard III, J. Computer-Aided Materials Design 8, 193 (2001)
- [189] P. Kwang-Oh, J.M. Sivertsen, J. Am. Ceram. Soc. 60, 537 (1977)
- [190] Z.P. Chang, E.K.Graham, J. Phys. Chem. Solids 38, 1355 (1977)
- [191] P. Pichet, H.K. Mao, P.M. Bell, J. Geophys. Res. 93, 15279 (1988)
- [192] M.J. Mehl, R.E. Cohen, H. Krakauer, J. Gephys. Res. 93, 8009 (1988)
- [193] P. Richet, H.K. Mao, P.M. Bell, J. of Geophysical Research 93, 15279 (1988)
- [194] T. Yamanaka, K. Kittaka, T. Nagai 97, 144 (2002)
- [195] H. Oda, O.L. Anderson, D.J. Isaak, I. Sizuki, Phys. Chem. Miner. 19, 96 (1992)
- [196] Y. Fei, Am. Mineral. 84, 272 (1999)
- [197] R.W.G. Wyckoff, Crystal Structure (Wiley, New York, 1963) 88
- [198] S. Spezial, C.S. Zha, T.S. Duffy, R.J. Hemley, H.K. Mao, J. Geophys. Res. 106, 515 (2001)
- [199] J.E. Jaffe, J.A. Snyder, Z. Lin, A.C. Hess, Phys. Rev. B 62, 1660 (2000)
- [200] M. Causa, R. Dovesi, C. Pisani, C. Roetti, Phys. Rev. B 33, 1308 (1986)
- [201] S. Israel, R. Saravanan, N. Srinivasan, S.K. Mohanlal, J. Phys. Chem. Solids 64, 879 (2003)
- [202] M. Matsui, J. Chemical Phys. 108, 3304 (1998)